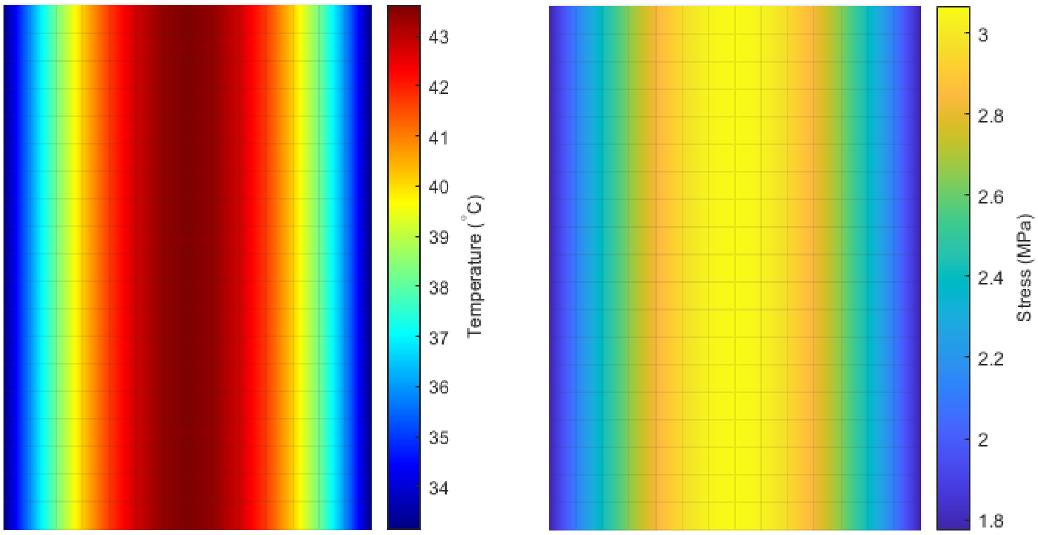

Thermal Cracking in Early-age Low-clinker Concrete

A Parametric Study on the Early-age Behavior of Concrete With Supplementary Cementitious Materials

Master's thesis in Structural Engineering and Building Technology

Erik Deborg
Victoria Jonasson

DEPARTMENT OF ARCHITECTURE AND CIVIL ENGINEERING
CHALMERS UNIVERSITY OF TECHNOLOGY
Gothenburg, Sweden 2026
deborg@chalmers.se
vicjona@chalmers.se

Master's thesis 2026

Thermal Cracking in Early-age Low-clinker Concrete

A Parametric Study on the Early-age Behavior of Concrete With Supplementary Cementitious Materials

ERIK DEBORG
VICTORIA JONASSON

Department of Architecture and Civil Engineering
Division of Structural Engineering
Chalmers University of Technology
Gothenburg, Sweden 2026

Thermal cracking in early-age low clinker concrete
A parametric study on the early-age behavior of concrete with supplementary cementitous materials
ERIK DEBORG
VICTORIA JONASSON

Supervisors: Carlos Gil Berrocal, Structural Engineering
Ingemar Löfgren, Thomas Concrete Group
Alexandre Mathern, NCC
Jonas Magnusson, NCC
Examiner: Carlos Gil Berrocal, Structural Engineering

Master's Thesis 2026
Department of Architecture and Civil Engineering
Division of Structural Engineering
Chalmers University of Technology
SE-412 96 Gothenburg
Telephone +46 31 772 1000

Cover: Stress and heat distribution through a wall section for an arbitrary concrete mix.

Typeset in LaTeX
Printed by Chalmers Reproservice
Gothenburg, Sweden 2026

Thermal cracking in hardening low-clinker concrete
ERIK DEBORG
VICTORIA JONASSON
Department of Architecture and Civil Engineering
Chalmers University of Technology

Abstract

This study is a master thesis at Chalmers University of Technology and aims to investigate which material parameters have the greatest impact on early-age thermal cracking in low-clinker concrete. It is a continuation on previous research conducted by collaborators from Chalmers University of Technology, NCC, Thomas Concrete Group and RISE, who identified which material parameters have the greatest impact on thermal cracking in concrete with ordinary Portland cement. The same material model and constitutive relations were adopted in this study. Prior to the parametric analysis, a literature study was performed that provided important background information about the subject.

The input data was provided by Thomas Concrete Group and contained four different C35/45 concrete mixes. The four mixes had 0, 16, 32 and 50 % slag as part of the binder. This enabled analyzing the impact of slag content in the analysis. The model was validated to ensure reliability using the program Produktionsplanering Betong, a program developed for planning during construction of concrete structures. With the model verified and with material input data from Thomas Concrete Group, One-Factor-at-a-time (OFaT) analyses and Monte Carlo simulations were used to evaluate the influence and sensitivity of individual parameters on the development of temperature and stress in low-clinker concrete.

The results showed the binder content and the heat of hydration to be the parameters with the most significant impact on thermal cracking, regardless of the slag content. Furthermore, the results showed greater sensitivity to large variations of the most significant parameters the more slag the mix contained. When comparing the results to the previously mentioned study, the parameters considered to have the most impact were nearly the same. One major difference was that the thermal expansion and contraction coefficient showed larger impact on thermal cracking for the mixes studied in this thesis, whereas it was not among the parameters with the most impact in the previous study.

Keywords: thermal cracking, green concrete, low-clinker concrete, early-age thermal cracking, stress/strength ratio, One-Factor-at-a-Time analysis, Monte-Carlo simulation, stress development, heat development.

Termisk sprickbildning i grön betong under härdningsprocessen
ERIK DEBORG
VICTORIA JONASSON
Institutionen för arkitektur och samhällsbyggnadsteknik
Chalmers Tekniska Högskola

Sammanfattning

Denna studie är ett examensarbete vid avdelningen för konstruktionsteknik på Chalmers Tekniska Högskola. Syftet med uppsatsen är att undersöka vilka materialparametrar som har störst inverkan på termisk sprickbildning i klimatförbättrad betong under härdningsprocessen. Arbetet är ett fortsättningsprojekt på tidigare forskning från Chalmers Tekniska Högskola, Thomas Concrete Group, NCC och RISE, där materialparametrarna med störst påverkan på termisk sprickbildning i betong med vanlig anläggningscement undersöktes. Projektet syftar till att använda samma numeriska modell och materialsamband som i det tidigare projektet för att resultaten skulle bli jämförbara. Som grund till projektet gjordes initialt en litteraturstudie där viktig information om ämnet fastställdes.

Materialdatan för projektet är framtagen av Thomas Concrete Group och Luleå Tekniska Universitet och bestod av fyra olika betongsammansättningar i hållfasthetsklass C35/45. Blandningarna innehöll 0, 16, 32 och 50 % slagg som alternativt bindemedel. Detta gjorde det möjligt att analysera påverkan av halten slagg i sammanhanget. Modellen verifierades med hjälp av Produktionsplanering Betong, ett program som är skapat för planering av betonggjutningar i produktionsstadiet. Detta gjordes för att säkerställa att modellen beräknar spännings- och temperaturutvecklingen på ett korrekt sätt. När modellen verifierats kunde materialdatan från Thomas Concrete Group användas för de parametriska analyserna. Dessa var en-faktor-i-taget analyser och Monte Carlo simuleringar och beräknade på olika sätt känsligheten hos alla parametrar och hur de individuellt påverkar termisk sprickbildning i ung, grön betong.

Resultaten visade att bindemedelshalten och hydratationsvärmen genomgående var de parametrar med störst inverkan på termisk sprickbildning, oavsett mängden slagg. Vidare visade resultaten högre känslighet för stora variationer av dessa parametrar för ökad mängd slagg. Vid jämförelse med resultaten från den tidigare studien visar sig de parametrar med störst påverkan vara näst intill desamma. En betydande skillnad var att den termiska expansions- och kontraktionskoefficienten visade större påverkan på sprickbildningen för de sammansättningar som analyserades i denna studie, medan den inte var lika betydande i det tidigare projektet.

Nyckelord: termisk sprickbildning, klimatförbättrad betong, termisk sprickbildning i ung betong, spänningskvot, en-faktor-i-taget analys, Monte-Carlo simulering, spänningsutveckling, värmeutveckling.

Acknowledgements

This master thesis has been carried out at Chalmers University of Technology, at the department of Structural Engineering and Building Technology and at the division of Structural Engineering. The project was conducted in collaboration with Chalmers, Thomas Concrete Group and NCC. We want to express our greatest gratitude to Carlos Gil Berrocal for being the examiner to this project and for sharing his knowledge in the subject. Thank you for valuable advice and for great supervision throughout the project.

We also want to extend our sincere thanks to our supervisors, Ingemar Löfgren at Thomas Concrete Group as well as Alexandre Mathern and Jonas Magnusson at NCC. Thank you for great discussions, useful feedback and for contributing with your expertise. A special thanks to NCC for providing us with great workspace at your office.

Erik Deborg & Victoria Jonasson, June 2026

List of Acronyms

Below is the list of acronyms that have been used throughout this thesis listed in alphabetical order:

CO_2	Carbon dioxide
MC	Monte Carlo
NaN	Not a Number
OFaT	One Factor at a Time
OPC	Ordinary Portland Cement
PPB	Produktionsplanering Betong
SCM	Supplementary Cementitious Material
TSTM	Temperature-Stress-Testing-Machine
w/b	Water to binder ratio

Nomenclature

Below is the nomenclature that have been used throughout this thesis.

Greek lower case symbols

α_{ct}	Stress/strength ratio limit value
α_T	Thermal expansion and contraction coefficient
β_T	Maturity factor
β_1	Tensile strength adjustment parameter
ε_{su}	Shrinkage parameter
η	Thermal crack risk
η_E	Modulus of elasticity adjustment parameter
η_{SH}	Shrinkage development parameter
θ	Part of maturity equation
θ_{ref}	Activation energy parameter
κ	Thermal conductivity
κ_1	Hydration heat parameter
κ_3	Activation energy parameter
λ_1	Hydration heat parameter
ρ	Density
σ	Stress

Greek upper case symbols

ϕ	Creep function adjustment parameter

Roman lower case symbols

c	Specific heat capacity
d	Creep function adjustment parameter
$d\varepsilon^0$	Increment of stress-independent strain due to temperature and shrinkage
$d\overline{\varepsilon^0}$	Average stress-independent strain increment
f_{ct}	Tensile strength
$f_{ct,28d}$	Tensile strength at 28 days
h_{conv}	Convection coefficient
$n_{cc,28d}$	Strength development parameter
p	Creep function adjustment parameter
q_{conv}	Heat transfer to/from the concrete surface
s	Strength development parameter
t	Time
t_e	Equivalent time
t_s	Setting time
$t_{s.sh}$	Time for start of autogenous shrinkage
t_{s1}	Shrinkage time development parameter
t_0	Retardation time
t_1	Hydration heat parameter
v	Wind velocity

Roman upper case symbols

C_C	Binder content
E	Modulus of elasticity
$E_{c,28d}$	Modulus of elasticity at 28 days
J	Creep compliance
Q_h	Rate of heat development
R	Relaxation function
R_{ext}	External degree of restraint
S	Crack risk safety factor
T	Concrete temperature
T_{amb}	Ambient temperature
T_{c0}	Initial concrete temperature

T_{surf}	Concrete surface temperature
W_u	Final heat of hydration

Contents

List of Figures

List of Tables

1
Introduction

This chapter introduces the topic of the project by describing the background, purpose and research question as well as a brief description of the method used. In addition, the limitations for the project as well as aspects from ethical, societal and ecological perspectives are described.

1.1 Background

With today's challenges of global warming, there is an urgent need to reduce the emission of carbon dioxide globally as well as on a national level. The construction sector accounts for 22% of Sweden's total carbon dioxide emissions and there are many areas of improvement that could lower the sectors environmental impact. Concrete is a cornerstone of Swedish building practice but Portland-cement, which is the most commonly used binder in concrete, and its production alone stands for 4% of the total CO_2-emissions in Sweden (Boverket, 2025).

Concrete is a widely used building material because of its durability and structural performance, especially suitable for bridges and tunnels, but the industry demands more sustainable building materials. In order to still utilize the advantages of concrete as a building material, it is vital to reduce the CO_2-emissions of cement production. This can be done by substituting part of the cement with alternative binders, such as slag and fly ash (Naturskyddsföreningen, 2022). Although this technical solution exists, there is still a lack of standardized procedures and knowledge of the material's early-age structural performance (Hedlund, Wiberg, Nilsson, & Persson, 2023a).

During the design process of large concrete structures, such as bridges and tunnels, the design engineer faces multiple challenges and requirements. One of them is to assess and reduce the risk of early-age thermal cracks by limiting the stress/strength ratio. In Sweden, Concrete Temperature & Stress (ConTeSt) is a widely used software for early age thermal cracking. More recently, Produktionsplanering Betong (PPB) has been introduced as an alternative, though it is based on similar material models and analysis techniques. ConTeSt has a database with several concrete mixes, but lacks information regarding low-clinker concrete mixes. Supplementary cementitious materials (SCMs) used in low carbon emission concrete cause a change in the hydration process, leading to modified time-dependent mechanical and thermal properties.

In order to provide material data for thermal cracking risk simulations and to obtain material parameters, extensive testing is required. Low-clinker concrete mixes are continuously developing, and in order to adapt these concrete mixes efficiently, it would be valuable to investigate which parameters (external and internal) have the greatest influence on early-age cracking in concrete with supplementary cementitious materials.

In 2022, a group of researchers with representatives from Chalmers University of Technology, NCC, Thomas Concrete Group and RISE started a project assessing the most significant parameters in a regular Portland-cement concrete with respect to thermal cracking. During that project, 22 different parameters and their impact on heat development and stress/strength ratio (directly representing the risk of cracking) was investigated numerically, by varying them in different ways and investigating the correlation to the results (Berrocal et al., 2024). This master's thesis was conducted as a continuation of that project, adapting the model and implementing material parameters but for low-clinker concrete. The project was carried out in collaboration with Chalmers, Thomas Concrete Group and NCC.

1.2 Purpose

This master's thesis aims to gain a deeper understanding of the thermal cracking behavior of low-clinker concrete at an early age. More specifically, the goal is to find which parameters have the greatest impact on heat development and thermal cracking risk during the curing period of concrete with supplementary cementitious materials. Such concrete mixes are constantly developing, and extensive lab testing is needed to determine the behavior of it. The results of this thesis are accordingly expected to identify the parameters with the most severe impact on the thermal cracking risk. The results could thereby suggest what tests and parameters to prioritize when developing new mixes.

1.3 Problem definition

Based on previously stated background and purpose, three main research questions are defined for the thesis and are enumerated below.

- What parameters have the most influence on early-age thermal cracking in low-clinker concrete?
- Are the parameters with the most influence on early-age thermal cracking the same in low-clinker concrete as for regular concrete?
- How does the percentage of supplementary cementitous material influence the structural and thermal response of concrete?

1.4 Limitations

The phrase "low clinker concrete" in this project refers to concrete where part of the cement is substituted with slag, unless otherwise stated. Hence, other supplementary cementitious materials was not covered in the analyses of this project. Moreover, the chemical aspect of hardening concrete and the reactions related to it was not addressed. This is since the thesis was made within the field of structural engineering and foucsed on the thermal and mechanical part of the material.

Due to previously unresolved issues associated with the use of DIANA for this type of parametric study (Berrocal et al., 2024), the study was instead carried out in Matlab. A script was implemented during the previously mentioned project and was also used in this thesis. Berrocal et al. states a number of limitations and assumptions which naturally applied in this project (Berrocal et al., 2024), such that the implemented model did not account for reinforcement amount.

Luleå University of Technology has, in collaboration with Thomas Concrete Group, conducted tests on low-clinker concrete and presented material parameters for concrete-mixes with varying contents of slag (Nilsson et al., 2024b)(Nilsson et al., n.d.). Consequently, the concrete recipes studied in the parametric study was limited to the relevant material data from these tests.

It is important to mention that the parameter C_c was cement content in the previous study, but was changed for this thesis to binder content. This was done to also include the SCM in the calculations. Accordingly, the assumption was made that the equations for calculating temperature, stress and strength development of OPC also apply for a combination of OPC and SCM.

1.5 Method

The project was carried out in three main parts. The first part was a literature study to gain knowledge about the subject and state a relevant foundation for decision making and analyzing results. In addition, the state-of-the-art was clearly defined by reviewing the most relevant and recent research within the field. The second part was a parametric study, varying one factor at the time to simulate the impact of each parameter. The third part was a sensitivity analysis to investigate the impact of each parameter in a realistic size spectra of variation. The latter was relevant since varying all parameters with the same fraction of the reference value might be unrealistically high or insignificantly low for certain parameters (Berrocal et al., 2024).

1.5.1 Literature study

To gain knowledge about the subject and to find relevant information for the analysis, a literature study was performed. To obtain an understanding of what material parameters are relevant and reliable, the concrete testing procedure and different supplementary cementitious materials was investigated as well as a summary of the available material data for different types of low-clinker concrete mixes. Previous research on the subject and today's standards and demands was reviewed in order to obtain an overall view of today's need.

1.5.2 Validation of model

Prior to running the main parametric study, it is of great importance to validate the model and confirm its reliability. This was done through running the material model using reference values for the complete set of parameters and compare the results to the program PPB. The comparison was done with respect to strength and heat development, representing the reference concrete behavior. The implemented material model was assumed to be realistic and reliable if the results correspond well to PPB.

1.5.3 Parametric study

The parametric study was done as a One-Factor-at-the-time (OFaT) analysis, implementing the Matlab program produced by Berrocal et al., 2024. OFaT analysis refers to varying one factor at the time to see the impact of all parameters studied on the results individually. In this particular case, the parameters studied are stated in Table 1.1.

Table 1.1: Parameters to be analyzed in the study and their unit.

Variable	Unit	Description
C_c	$[kg/m^3]$	Binder content
W_u	$[J/kg]$	Final hydration heat
t_1	$[h]$	Hydration heat parameter
κ_1	$[-]$	Hydration heat parameter
θ_{ref}	$[K]$	Activation energy parameter
κ_3	$[-]$	Activation energy parameter
T_{c0}	$[°C]$	Initial concrete temperature
$f_{ct,28d}$	$[MPa]$	Mean tensile strength
s	$[-]$	Strength development parameter
t_s	$[h]$	Setting time
$n_{cc,28d}$	$[-]$	Strength development parameter
β_1	$[-]$	Tensile strength adjustment parameter
$E_{c,28d}$	$[GPa]$	Modulus of elasticity
η_E	$[-]$	Modulus of elasticity adjustment parameter
ϕ	$[-]$	Creep function parameter
d	$[-]$	Creep function parameter
p	$[-]$	Creep function parameter
ε_{su}	$[-]$	Shrinkage parameter
η_{SH}	$[-]$	Shrinkage development parameter
α_T	$[(°C)^{-1}]$	Thermal expansion coefficient
h_{conv}	$[W/m^2K]$	Convection coefficient
R_{ext}	$[-]$	External degree of restraint

Berrocal et al. chose to keep certain parameters constant throughout the simulation. The reason for this was that those parameters are assumed not to vary in a significantly large enough range in regular concrete, and at the same time reduce the total number of parameters for the analysis (Berrocal et al., 2024). All parameters assumed constant are visualized in Table 1.2. Important to mention is that even though some parameters are not part of the parametric study, they may vary between the different concrete mixes.

Table 1.2: Parameters assumed to be constant and their unit.

Variable	Unit	Description
ρ	$[kg/m^3]$	Density
c	$[J/(kg°C)]$	Specific heat capacity
k	$[W/(m°C)]$	Thermal conductivity
λ_1	$[-]$	Hydration heat parameter
t_{s1}	$[h]$	Shrinkage time development parameter
$t_{s.sh}$	$[h]$	Time for start of autogenous shrinkage

In the analyses, the parameters varied +/- 20% in steps of 5% units. This is in line with the study done by Berrocal et al. (2024) to be able to directly compare the results. As mentioned previously, what initiates a thermal crack are directly linked to the temperature and the residual tensile stresses. Accordingly, the results analyzed were maximum concrete internal temperature as well as stress/strength ratio.

1.5.4 Monte Carlo simulation

Monte Carlo simulations was performed to determine the impact of the parameters in a large number of statistically possible concrete mix combinations. Monte Carlo simulation is a type of sensitivity analysis based on randomized input (Wahnström, 2017). In this particular case, the idea of running this kind of simulation is to investigate the impact of each parameter in possible mixes apart from the reference concrete. To do this, the statistical distribution of each parameters value was stated and the simulation allowed the parameters to vary only within this interval. This calculated results with more realistic input since, as mentioned, varying the value with +/- 20 % might be unrealistically large for certain parameters and at the same time insignificantly small for others.

1.6 Risk assessment

In accordance with the department's instructions for master theses, a risk assessment has been conducted. This was made since the project will partly be carried out outside of Chalmers campus. Accordingly, the risk assessment mainly focuses on the safety regulations of the NCC office. The risk assessment is presented in Appendix A.

1.7 Societal, ethical and ecological aspects

With urban development taking place globally, the world is in constant need of developing existing building materials. This to meet structural, economical and environmental demands. From a social perspective, the topic of thermal cracking might not be a direct issue. However, limiting concrete cracking in general is of great importance for the serviceability of concrete structures. Although a cracked concrete structure, in some cases, is perfectly appropriate from a structural perspective, people might feel uncomfortable approaching the structure, and crack limiting is therefore essential. In addition, thermal cracking might defect the impression of the structure aesthetically.

Furthermore, limiting cracking of concrete structures is important for the durability of the structure. This is due to that it decreases the risk of reinforcement corrosion due to water penetration, and at the same time limiting water leakage. Therefore, assessing the parameter with the most influence on thermal cracking can be useful for future concrete design. It can reduce the overall cracking and increase the serviceability of the material, in some way counteracting the need of renovation and new buildings.

The acceleration of urban expansion naturally relates to an ecological perspective of material research. With the current state of the environment and the fact that the environmental debate is highly on the agenda in society, it is of great relevance that the building sector aims to reduce carbon emissions. One way of achieving this is through low-clinker concrete, referring to concrete with complementary cementitious materials, due to the climate impact of cement. That said, reducing the cement content implies certain challenges and will affect the properties of the material, which is why research on low-clinker concrete is important.

From an ethical perspective, the topic relates to the broader discussion on the environmental impact of concrete and the need to reduce its carbon footprint in construction. Although the binder is partly substituted with complementary cementitious materials, concrete could still be considered a material with large environmental impact. In addition to the ethical point of view, but despite the project topic, it is important to develop such project in a correct way. As mentioned, this project is a continuation of the project by Berrocal et al. (2024), and will be based on the same procedure but implemented for other types of concrete mixes. This means that the material model created in that project will be used as a base for this masters thesis but modified and adjusted. Hence, the credit for the origin of the material model does not belong to this master thesis but solely to Berrocal et al. (2024). Lastly, the quality of data used for the analysis are assumed to be sufficiently accurate.

2
Literature Study

The following chapter is a literature study. It covers relevant theory behind the topic to be used as a base for the later parametric study. Information about cement and cementitious materials, strategies for simulation and testing of concrete as well as current demands regarding heat development and crack widths are stated. In addition, the state of the art is established to clarify the current situation of the topic.

2.1 Cement and supplementary cementitious materials

The main binder in regular concrete is Ordinary Portland Cement (OPC) and is well used globally. In the hydration process, the cement reacts with water and solidifies, creating the binding material of which concrete relies on. The hydration is a quick process in the early age of concrete and slows down as time passes. The main, current, drawback of Portland cement is its carbon footprint which is why the concrete industry nowadays replace parts of it with supplementary cementitious materials (SCMs), something which has a large impact on thermal and mechanical properties and their development over time (Taylor, 2013).

There are several types of SCMs and ongoing research on new ones. Fly ash, slag, volcanic ash and silica fume are four examples of such materials. Silica fume is a material deriving from the smelting process of silica and ferrosilicon. Its material structure is an extremely fine powder, often 100 times finer than regular cement. This together with the high content of silica makes the material pozzolanic and highly reactive. It is known that concrete with silica fume as part of the binder enhances the mechanical properties due to improvement the bond between the mortar and aggregate. Addition of silica fume also decreases the possibility of chloride ingress which increases the durability of the concrete it is used in (Khan & Siddique, 2011). However, it is also known to increase the autogenous shrinkage and thereby the cracking risk (Wan et al., 2022).

Volcanic ash is a material occurring when lava from volcanic activity cools rapidly and hardens. If ground into a fine powder, the material obtains pozzolanic properties when used together with cement. The great advantage of volcanic ash as a SCM is that it will keep on producing itself as long as there are active volcanoes which can be useful for improving the carbon footprint of concrete (Löfgren, 2024). However, the compressive strength is affected negatively in certain mix proportions. For such mixes, volcanic ash can reduce the elastic modulus of the concrete, with direct impact on other mechanical properties such as tensile strength (Pinto-Almeida et al., 2025).

Fly ash is a by-product from the coal energy plants. It occurs by burning the coal which to a great extent contains rock materials. During the burning process, the unwanted (for production of energy) rock material melts and as it cools again, it converts into a powder similar to cement. The obtained material contains silica, a material which is reactive in contact with calcium hydroxide. The calcium hydroxide emerges from the hydration process of PC which is why fly ash can be used as a SCM. This process is known as a pozzolanic reaction (Taylor, 2013).

For concrete with fly ash as part of the binder, the setting time is generally longer compared to using only PC. Although, it will continue for a longer period of time, leading to improved long-term structural performance of the concrete. Another change in long term behavior is the permeability which will decrease when using fly ash. This essentially means lower risk of water penetration and therefore greater durability (Taylor, 2013).

Slag is a by-product but from the iron industry. Slag derives from melting iron ore into pure iron, and the material occurs by adding a fluxing agent to the melting process. This removes impurities and slag forms as a paste inside the blast furnace above the iron. By passing the paste through a cold stream of water or air, slag is created. For small cement replacements, concrete incorporating slag yields a similar material behavior as pure PC concrete. However, increasing that ratio, the speed of strength development decreases, but simultaneously develops over a longer period of time. The latter can thereby induce greater long-time strength, but weaker behavior in early ages (Taylor, 2013). Further on for this project, slag will be the SCM focused on.

2.2 Concrete testing

Modeling the early-age thermal and mechanical behavior of concrete typically involves the use of different analytical expressions that describe the different physical processes taking place during the concrete hydration. Theses equations use a lot of parameters that need to be calibrated for each concrete mix, most often through experimental testing. Consequently, the following part contains descriptions of the different tests.

Compressive strength
The development of compressive strength can be obtained by casting standardized specimens and simply loading them to compressive failure at different stages of curing. Apart from testing cubes cured in specifically selected high and low temperatures, it has to be done in reference temperature of 20 $°C$ to be able to evaluate the reference strength development. By doing this, it is also possible to evaluate the maturity function and equivalent curing time (Berrocal et al., 2024).

Heat development
The heat development of a specimen can be determined by casting it into a semi-adiabatic calorimeter. This is an insulated container in which the concrete specimen is placed and where the temperature development is recorded. As soon as the concrete is poured and compacted in line with the standards and the temperature sensor is placed, the calorimeter is closed and the temperatures are recorded as the specimen cures (SIS, 2018).

Creep
Creep coefficients can be obtained by applying constant load to specimens over time and meanwhile measure the deformation. The creep data can also be converted into relaxation spectrum which can be used for further stress and stiffness calculations in during hardening (Nilsson et al., 2024a).

Free movement
Free movement refers to the movement of concrete without external loading, but with a controlled temperature rise corresponding to that in the temperature stress testing machine. This data is obtained by measuring deformation and change in length for a specimen placed left to cure on its own without external impact. The measurements will generate data for both thermal deformation as well as autogenous shrinkage (Nilsson et al., n.d.).

Temperature-stress testing machine
Another way of monitoring the early age behavior of concrete is through a temperature stress testing machine (TSTM). A TSTM can be used for both direct measuring of material behavior, but also to validate data obtained through other types of tests (Berrocal et al., 2024). The TSTM consists of a formwork and several mechanisms attached to it to monitor the behavior. It uses two thermocouples casted into the sample to record the heat development and the concrete temperature during curing (Nguyen et al., 2019).

One end of the specimen is fully locked in place, while the other side is movable and connected to a recovery motor, adjusting the amount of restraint in the specimen. Two bars are attached along the axis of loading and as the specimen shrinks, the bars experiences equal shortening. The bars are attached to a transducer, recording displacement and sending feedback to the recovery motor. This is done so that the specimen experiences constant restrain throughout the process. The side with the recovery motor also controls the amount of loading of the specimen (Nguyen et al., 2019).

2.2.1 Available material data

Today there is material data available for a limited amount of concrete mixes with varying amount of SCM, with material parameters obtained as described previously. Thomas Concrete Group tested four mixes with varying amount of slag including a reference mix. The mixes are presented in Appendix B, Figure B.1, and will be the ones used for this study.

2.3 The process of early age thermal cracking

Cracking in concrete can compromise the structural integrity and durability of the structure. Intact concrete acts as a barrier that protects the reinforcement against corrosion-inducing agents, such as oxygen, moisture, and chloride ions. When cracking occurs, that barrier has lost its integrity, allowing corrosion-agents to penetrate more rapidly and initiates corrosion of the reinforcement (Berrocal et al., 2015). Cracking accelerates the corrosion-process and consequently reduces the service life of the structure. To minimize the risk of early-age thermal cracking and its consequences, it is important to know the reasons why cracking occurs in the first place.

The early-age thermal cracking process is partly driven by the hydration phase that occurs during the hardening of concrete. The hydration process is an exothermic process, where water is consumed and heat is emitted. The emitted energy from the hydration reaction (heat of hydration) increases the core temperature of the concrete, which leads to an increase in volume. However, if the concrete structure is restrained from this kind of movement in some way, the volume change leads to compressive strains. Autogenous shrinkage is due to the water consumption during the hydration process which eventually lead to self-desiccation. When the concrete specimens internal temperature later on decreases during the cooling phase in combination with autogenous shrinkage, tensile strains and stresses appear (Nilimaa et al., 2017).

In cases where the tensile strain exceeds the capacity of concrete, thermal and shrinkage cracks appear (Qu et al., 2024). Thermal expansion and autogenous shrinkage caused by self-desiccation in combination with external restraint as well as environmental effects are the main reasons for cracking during the hardening of concrete. The type of crack that emerge during the heating and cooling phase are surface and through cracks respectively (Nilsson et al., 2024c). The heating and cooling phase take place during the first 1-2 weeks (Ji, 2008) and the effect on stresses within the hardening concrete can be seen in figure 2.1. The heat emitted during the hydration process (heat of hydration) is directly influenced by some of the parameters analyzed in this report, subsequently influencing the risk of cracking.

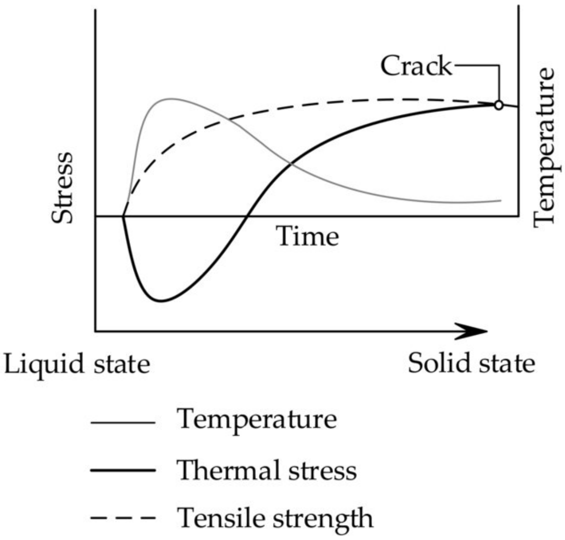

Figure 2.1: Generalized temperature and stress development in early-age concrete (Longlong et al., 2018).

Autogenous shrinkage is due to the consumption of water due to the hydration reaction while drying shrinkage is due to the evaporation of water. Although autogenous shrinkage have the greatest impact on early-age cracking, drying shrinkage can lead to further expansion of the cracks (Qu et al., 2024). The ambient temperature, relative humidity and wind velocity influences the evaporation of water and hence the drying shrinkage.

Environmental conditions also have an impact on the early-age cracking process. Higher temperature differences between internal and external temperatures induce thermal strains and can cause surface cracking at an early age. When the ambient temperature drops below zero, frost cracking can occur due to freezing and expansion of the water within the concrete. If the ambient temperature varies above and below the freezing point of the water, the freeze and thaw process leads to an uneven distribution of internal stress (Qu et al., 2024). Thermal expansion or contraction due to the ambient temperature leads to thermal strains within the concrete structure that can result in temperature induced cracking.

All of the reasons for cracking are connected to each other, making it a complex process. For example, lowering the water-to-binder ratio (w/b) increases the compressive strengths and decrease the drying shrinkage. However, if the w/b is below 0.42 it increases the self-desiccation and consequently increases the autogenous shrinkage. A too high w/b is reason for more bleeding water and increases the risk of settlement cracking.

The early-age cracking process is a well studied subject with continuous research progress all over the world. Publications on the subject of thermal cracking go back to 1920 and the first study conducted in Sweden was by Löfquist studying the thermal effects in hardening concrete (Löfquist, 1946). In 1990, the interest in the subject got renewed which resulted in further studies regarding the hydration, structural, thermal, and viscoelastic behavior of young concrete as well as the development of numerical analysis tools (Berrocal et al., 2024). More recently, studies have been conducted on how SCM effects the behavior of concrete, especially regarding early-age cracking. SBUF have funded projects that have been valuable in moving towards the adaption of low-clinker concrete, including

- 13872 Grönare anläggningsbetong - data för temperatur- och härdningsstyrning (2023b),
- 14096 STAR - Temperatursprickdata för klimatförbättrad betong (2023),
- 14155 Mätningar av töjningar i ung klimatförbättrad betong (2024).

These reports have resulted in material properties, standardized cases and development of crack mitigation methods for hardening concrete with SCMs.

2.4 Swedish standards and demands

The thermal crack risk, η, can be calculated as the ratio between the calculated tensile stress at and the tensile strength at a certain time. Alternatively, the ratio between the tensile strain and the ultimate tensile strain at a certain time can be used. If the risk of thermal cracks is too high, AMA Anläggning provides guidelines to mitigate the risk of cracking. There are three types of calculations methods regarding crack control that can be found in AMA Anläggning (2023).

Method 1 focuses the limitation of surface cracks by limitation of the surrounding temperature, heat development within the structure, binding materials, w/b_{ekv}, size of casting segments, and demolding. The conditions that need to be fulfilled are listed below.

- The cement content (including SCM) < 460 kg/m^3
- SCM $< 20\%$.
- w/$b_{ekv} \geq$ 0,38
- The thickness of the structure $<$ 1,2 m
- The intitial temperature should be between 10°C and 25°C
- The ambient temperature during casting until demoulding should be between 5°C and 20°C
- The temperature of adjacent castings should be higher or equivalent to the ambient temperature.
- Earliest time of demoulding is four days after casting.

Method 2 used standardized cases provided by Luleå Technical University (Emborg et al., 1997). This method is only valid when the ambient temperature is above 0.

Method 3 refers to calculations performed with a analysis software, alternatively, "Handboksmetoden", CraX1. This method requires proven and reliable input data.

In all cases, it is important to fulfil the demands given in SS-EN 13670 and SS 137006 regarding the development of heat during the hardening of concrete. The temperature within the concrete structure should not exceed 70°C.

In an effort to meet the demand for more environmentally friendly concrete, some adjustments to the demands and guidelines were made in the latest edition of AMA Anläggning. However, the allowed amount supplementary cementitious material is limited to 20% for method 1 and 2 (Hedlund, Wiberg, Rasmark, et al., 2023). For concrete with more than 20% supplementary materials method 3 may be used with either recipe specific material parameters or general material parameters. The exposure class together with the cement content and type of material parameters dictates the minimum crack risk safety factor, S, should be used according to AMA anläggning in Table 2.1 and Table 2.2 where S is equivalent to $1/\eta$.

Table 2.1: Saftey factors, S, for calculation method 2 and 3 (Byggtjänst, 2023).

Exposure class	**Recipe specific material parameters**	**General material parameters**	
		Cement content, kg/m^3	
		≤ 460	> 460
XC1, XC2	1,05*	1,18	1,33
XC3, XC4	1,11	1,25	1,42
XD1, XD2, XS1, XS2	1,18	1,33	1,54
XD3, XS3	1,25	1,42	1,67

*S is calculated as the ratio between tensile stress and tensile strenght.

Table 2.2: Saftey factors, S, for calculation method 3 for structures subjected to one-sided water pressure (Byggtjänst, 2023).

Exposure class	**Recipe specific material parameters**	**General material parameters**	
		Cement content, kg/m^3	
		≤ 460	> 460
All	1,42	1,67	2,0

The type of material parameters refers to the degree to which a certain concrete mix is tested. The specific material parameters are fully tested and allow a lower crack risk factor while the general material parameters calls for a higher crack risk factor, resulting in increased measures and costs for the project (Hedlund, Wiberg, Nilsson, and Persson, 2023b).

3

Method

The main purpose of the thesis was to perform One Factor at the Time (OFaT) analyses as well as a Monte Carlo simulations on the four mixes from Thomas Concrete Group. This was done with the numerical model implemented by Berrocal et al. (2024) but with different concrete recipes. Prior to running the main analysis, the model had to be verified to make sure the results was trustworthy.

3.1 Model setup

The model was set up as a slice in the center of a 700 mm thick wall. In order to perform a 2D-analysis, the section is presumed to be sufficiently far away from the top and bottom of the wall so the thickness of the studied part can be disregarded. The analyzed geometry will therefore be a 700 mm wide 2D-element with partial restraints boundary conditions at the edges perpendicular to the length of the wall and thermal boundary conditions on the edges along the side surfaces of the wall, where it is free from restraints according to Figure 3.1. Convective heat transfer conditions are applied on the walls thermal boundaries according to Equation 3.1.

$$q_{conv} = h(T_{surf} - T_{amb}) \tag{3.1}$$

where

$$\begin{aligned}
&q_{conv}\ [W/m^2] - Heat\ transfer\ to/from\ the\ surface \\
&h\ [W/m^{2\circ}C] - Heat\ transfer\ coefficient \\
&T_{surf}\ [^\circ C] - Concrete\ surface\ temperature \\
&T_{amb}\ [^\circ C] - Ambient\ temperature
\end{aligned}$$

The ambient temperature was decided to be constant 20°C for all analyses and the heat transfer coefficient was calculated according to Equation 3.2.

$$h = \begin{cases} 5.6 + 3.95v & if\ v \leq 5\ m/s \\ 7.8v^{0.78} & if\ v > 5\ m/s \end{cases} \tag{3.2}$$

where

$$v\ [m/s] - Wind\ velocity$$

Since the model disregards formwork, the heat transfer coefficient only depends on the wind velocity. Assuming a velocity of 1 m/s the heat transfer coefficient is calculated to 9.55 $W/m^{2\circ}C$.

With a distance of 0.05 m between the nodes across the studied slice and the studied wall being 0.7 m thick, the analysis used 15 nodes across it. The calculations were made for the first eight nodes, simplifying the modeling and the results from the first seven nodes was then mirrored as also being node nine to fifteen with the assumption that the heat, stress and strength develops symmetrically in the center node along the wall.

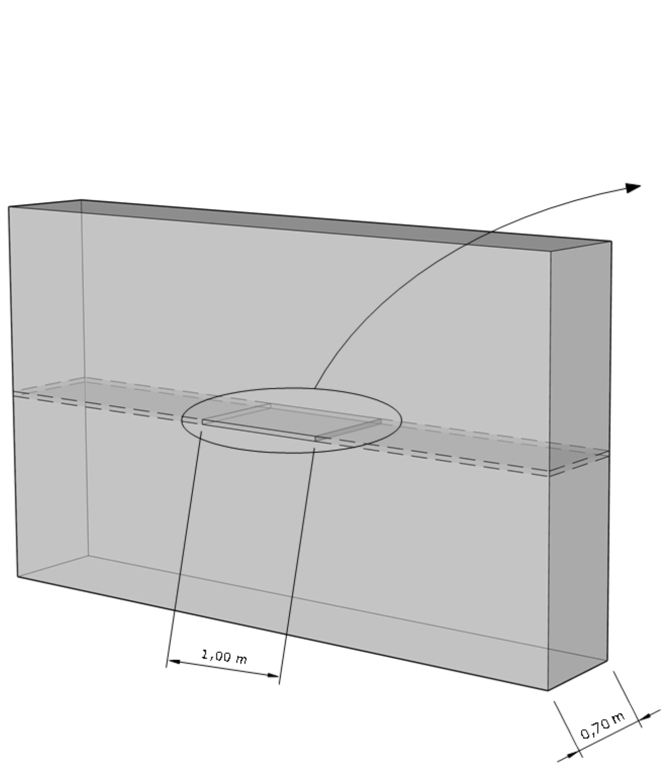

Figure 3.1: Geometry and boundary conditions of model.

3.1.1 Constitutive relation and material properties

This chapter elaborates the equations used to model the early-age material behavior. All equations are in some way related and used to calculate the development of stress, strength and heat. This is due to that the main analysis will consider the stress-to-strain ratio and heat development. The analysis first uses a finite difference model to calculate the heat development throughout the wall. The results of the thermal analysis are then used to calculate the stress and strength history.

Heat development

First, a thermal analysis is performed to obtain the variation and history of temperature throughout the wall. Since the top and bottom boundaries can be assumed adiabatic, the problem can be reduced to a 1D-analysis, in accordance with Equation 3.9.

$$\kappa \frac{\partial^2 T}{\partial x^2} + Q_h(t) = \rho c \frac{\partial T}{\partial t} \tag{3.3}$$

where

$$\kappa\ [W/m \circ C] - Thermal\ conductivity$$
$$Q_h\ [W/m^3] - Rate\ of\ heat\ development$$
$$\rho\ [kg/m^3] - Density$$
$$c\ [kJ/kg \circ C] - Specific\ heat\ capacity$$

The temperature development within the structure could then be used to determine the mechanical behavior of a certain concrete mix in the early stage.

Heat of hydration

The equation for calculating generated heat of hydration (Q_u) as a function of kilograms hydrated binder is stated below.

$$Q_h(t) = W_u e^{-\lambda_1 \left(ln \left(1 + \frac{t_e}{t_1} \right) \right)^{-\kappa_1}} \tag{3.4}$$

where,

$$t_e\ [h] - Equivalent\ time$$
$$W_u\ [J/kg] - Final\ heat\ of\ hydration$$
$$\lambda_1\ [-] - Adjustment\ parameter$$
$$t_1\ [h] - Adjustment\ parameter$$
$$\kappa_1\ [-] - Adjustment\ parameter$$

Maturity

The factor β_T is a maturity factor and was used to calculate the equivalent time. The maturity factor is calculated using Equation 3.5.

$$\beta_T(t) = exp \left(\theta \left[\frac{1}{293} + \frac{1}{T(t) + 273} \right] \right) \tag{3.5}$$

with,

$$\theta = \theta_{ref} \left(\frac{30}{T + 10} \right)^{\kappa_3} \tag{3.6}$$

and where,

$$\begin{aligned} &\theta_{ref}\ [K]\ - Activation\ energy\ parameter \\ &\kappa_3\ [-]\ - Maturity\ parameter \\ &T\ [^{\circ}C]\ - Concrete\ temperature \end{aligned}$$

Equivalent time

The maturity parameter calculated in Equation 3.5 was then used to calculate the equivalent time according to

$$t_e = \int_0^t \beta_T dt \tag{3.7}$$

where,

$$t\ [h]\ - Time$$

Autogenous shrinkage

Autogenous shrinkage is the shrinkage of concrete due to the hydration of the binder, see section 2.3. The equation used for autogenous shrinkage was Equation 3.8.

$$\varepsilon_{sh}^0 = -\varepsilon_{su} exp \left(\left(-\frac{t_{s1}}{t - t_{s.sh}} \right)^{\eta_{sh}} \right) \tag{3.8}$$

where,

$$\begin{aligned} &\varepsilon_{su}\ [-]\ - Final\ value\ of\ autogenous\ shrinkage \\ &t_{s.sh}\ [h]\ - Time\ for\ start\ of\ autogenous\ shrinkage \\ &t_{s1}\ [h]\ - Shrinkage\ time\ development\ parameter \\ &\eta_{sh}\ [-]\ - Shrinkage\ development\ parameter \end{aligned}$$

Thermal strain

The thermal strain was calculated according to Equation 3.9.

$$\frac{\partial \varepsilon_{temp}^0}{\partial t} = \alpha_T \frac{\partial T}{\partial t} \tag{3.9}$$

where,

$$\alpha_T\ [^{\circ}C^{-1}]\ - Thermal\ expansion/contraction\ coefficient$$

Modulus of elasticity
The development of the elastic modulus was calculated according to Equation 3.10.

$$E_c = E_{c,28d}\ exp\left(s\left(1-\left(\frac{672-t_s}{t-t_s}\right)^{n_{cc,28}}\right)\right)^{\eta_E} \tag{3.10}$$

where,

$E_{c,28d}\ [GPa]\ -\ Mean\ elastic\ modulus\ at\ 28\ days$
$s\ [-]\ -\ Strength\ development\ parameter$
$t_s\ [h]\ -\ Setting\ time$
$n_{cc,28}\ [-]\ -\ Strength\ development\ parameter$
$\eta_E\ [-]\ -\ Modulus\ of\ elasticity\ adjustment\ parameter$

Tensile strength
The tensile strength was calculated using Equation 3.11.

$$f_{ct} = f_{ct,28d}\ exp\left(s\left(1-\left(\frac{672-t_s}{t-t_s}\right)^{n_{cc,28d}}\right)\right)^{\beta_1} \tag{3.11}$$

where,

$f_{ct,28d}\ [MPa]\ -\ Tensile\ strength\ at\ 28\ days$
$\beta_1\ [-]\ -\ Adjustment\ parameter$

Creep
Creep was calculated in the model with Equation 3.12.

$$\varphi = \left(\phi\ t_0^{-d}\,(t-t_0)^p\right) \tag{3.12}$$

where,

$\phi\ [-]\ -\ Adjustment\ parameter$
$t_0\ [h]\ -\ Retardation\ time$
$d\ [-]\ -\ Adjustment\ parameter$
$t\ [h]\ -\ Time$
$p\ [-]\ -\ Adjustment\ parameter$

The adjustment parameters ϕ, d and p was obtained by numerically changing the values several times until the smallest difference in stress to the results from PPB was found. The reason for this was that PPB uses the relaxation spectrum to model the creep behavior which can not be translated into one equation. It was therefore decided to adjust the model to the stress from PPB using a double power law for creep behavior. The values of these parameters are stated in Table 3.2 for each individual mix. Since calculating heat development is not affected by those parameters, they were set to arbitrary values to be able to perform those calculations.

Also related to creep is the creep compliance used for modeling the viscoelastic behavior of concrete prior to hardening. The creep compliance is based on a "Double Power Law" and was used to calculate relaxation as well as finding the adjustment parameters α, d and p of the general creep function (Berrocal et al., 2024). The equation used for creep compliance was

$$J(t, t_0) = \frac{1}{E_c}\left(1 + \phi\, t_0^{-d}\,(t - t_0)^p\right) \tag{3.13}$$

where,

$$E_c\ [GPa]\ - Modulus\ of\ elasticity$$

Stress-independent strain
Stress-independent strain refers to strain that occurs from other sources than external loading. In other words, strain that will occur regardless of whether the concrete structure is in service or not (Engström, 2007). The stress-independent strain was calculated from the thermal expansion and drying according to Equation 3.14.

$$d\varepsilon^0 = d\varepsilon^0_{temp} + d\varepsilon^0_{sh} \tag{3.14}$$

Stress
Considering the autogenous shrinkage, thermal strain, external restraint, and viscoelastic behavior, the stress variation in the concrete was calculated according to Equation 3.15.

$$d\sigma(t) = R(t, t_0)[(1 - R_{ext})d\overline{\varepsilon^0} - d\varepsilon^0] \tag{3.15}$$

where

$d\varepsilon^0\ - The\ increment\ of\ stress - independent\ strain\ due\ to$
$temperature\ and\ shrinkage$
$d\overline{\varepsilon^0}\ - Average\ stress - independent\ strain\ increment\ over$
$the\ cross - section$
$R_{ext}\ - External\ degree\ of\ restraint$
$R(t, t_0)\ [GPa] - Relaxation\ function\ that\ describes\ the\ viscoelastic\ behaviour$
$under\ constant\ sustained\ strain\ and\ is\ equal\ to\ the\ inverse\ of$
$the\ compliancefunction,\ J(t, t_0),\ in\ Equation\ 3.13.$

3.2 Concrete mixes

There were four different concrete mixes studied in this thesis, each with different amounts of slag as well as a reference mix with purely OPC. In Table 3.1, the proportions and materials for the mixes are stated, and in Table 3.2, the 22 parameters studied are presented for each mix. The mixes are the results of the experimental testing from Thomas Concrete Group and Luleå University of Technology by Nilsson et al. (n.d.).

Table 3.1: Mix proportions of the studied concrete mixes, w/b = 0.42 and strength C35/45 (Nilsson et al., n.d.).

Materials $[kg/m^3]$	**Mix 1, ref**	**Mix 2, 16% slag**	**Mix 3, 32% slag**	**Mix 4, 50% slag**
Cement Anl Brevik	320,0	266,6	214,2	156,1
Cement Anl Silte	80,0	66,7	53,5	39,0
Slag		63,3	125,8,0	195,1
Water	168,0	166,6	165,3	163,9
0/4 mm Sand	674,1	674,5	674,8	675,0
0/6 mm Fine aggregates	254,8	255,0	255,1	255,2
8/16 mm Coarse aggregates	870,6	871,2	871,5	871,8
Superplasticizer: MasterGlenium 592	2,400	2,38	2,36	2,34
Air entraining agent: MicroAir 105	0,400	0,397	0,394	0,39

Table 3.2: Material input for the concrete mixes with slag, w/b = 0.42 and strength C35/45 (Nilsson et al., n.d.).

Variable	**Unit**	**Mix 1, ref**	**Mix 2, 16% slag**	**Mix 3, 32% slag**	**Mix 4, 50% slag**
C_c	$[kg/m^3]$	400	396.6	393.5	390.2
W_u	$[J/kg]$	376 000	370 000	360 000	340 000
t_1	$[h]$	10.000	14.014	20.000	30.000
κ_1	$[-]$	1.271	1.24	1.150	1.010
θ_{ref}	$[K]$	4012	4092	4360	5040
κ_3	$[-]$	0.497	0.373	0.218	0.234
T_{c0}	$[°C]$	10 - 35	10 - 35	10 - 35	10 - 35
t_s	$[h]$	5	5	5	3
s	$[-]$	0.162	0.207	0.469	0.525
$n_{cc,28d}$	$[-]$	0.618	0.671	0.484	0.511
$f_{ct,28d}$	$[MPa]$	3.25	2.94	2.29	2.29
β_1	$[-]$	0.667	0.667	0.667	0.667
$E_{c,28d}$	$[GPa]$	34.3	33.4	35.2	33.9
η_E	$[-]$	0.5	0.5	0.5	0.5
ε_{su}	[-]	-141.36e-6	140.59e-6	-141.75e-6	-140.12e-6
η_{SH}	[-]	0.400	0.452	0.600	0.650
ϕ	$[-]$	2.8453	3.6582	1.6726	1.4766
d	$[-]$	0.3497	0.5879	0.2089	0.3242
p	$[-]$	0.3133	0.1277	0.2975	0.3107
α_T	$[(°C)^{-1}]$	11.968e-6	10.251e-6	10.770e-6	12.000e-6
h_{conv}	$[W/(m^2 °C)]$	9.55	9.55	9.55	9.55
R	[-]	0.83	0.83	0.83	0.83

3.3 Model verification

In order to verify the model, temperature and stress results for each mix was compared to a FEM-software. The most common numerical analysis tool used in Sweden for early-age cracking is ConTeSt (Nilsson et al., 2024c). It is a well proven and efficient FE-software that has been developed and improved over the last 20 years. Byggföretagen later developed Produktionsplanering betong (PPB) that is based on similar consecutive relationships and material models as ConTeSt. Lund University created a software called Hacon for the same purpose, though it is rather limited compared to ConTeSt and PPB. The precision of the FE-results is heavily influenced by the accuracy of the tested material parameters. Nilsson et al. (2024c) states that some FE-programs are flawed with regard to modeling the behavior of young concrete and that there is a need for improved quality control.

For this project, PPB was chosen as the verification tool due to its accessibility and compatibility with the test results. The model was set up in PPB with the same boundary conditions and material properties as the one modeled in Matlab. The model parameters obtained from the Thomas Concrete group (as stated in Table 3.2) and the calculated boundary conditions were used in the validation of the model.

Each concrete mix was evaluated using PPB and the numerical Matlab model. The heat development and stress development was extracted for initial temperatures ranging between 15°C and 30°C in steps of 5°C and compared in Figure 3.2, Figure 3.3, Figure 3.4 and Figure 3.5.

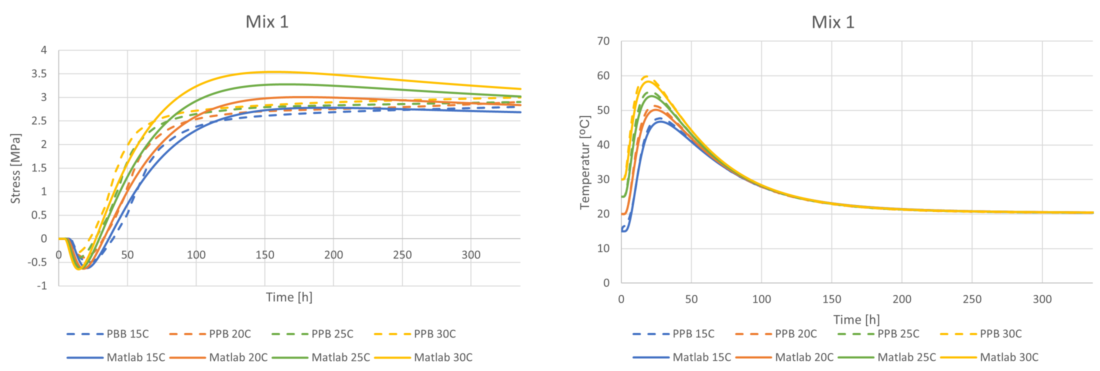

Figure 3.2: Comparison of temperature and stress development calculated with Matlab and PPB during the first 14 days for mix 1.

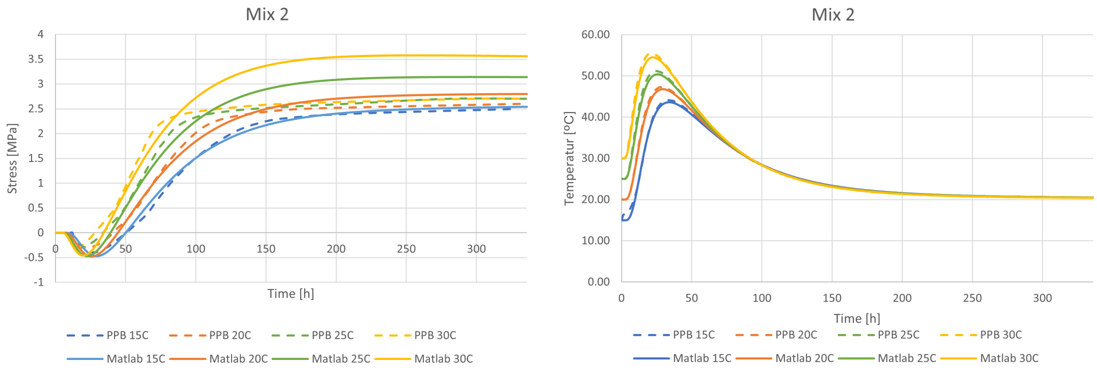

Figure 3.3: Comparison of temperature and stress development calculated with Matlab and PPB during the first 14 days for mix 2.

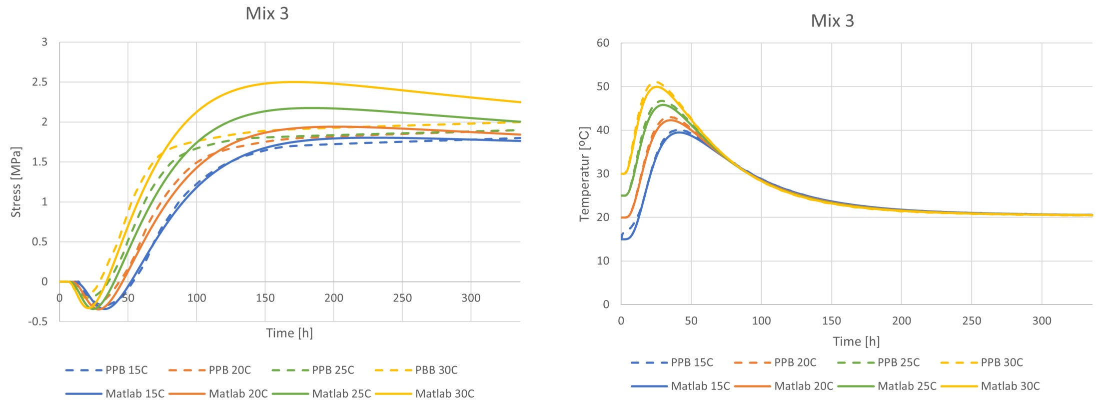

Figure 3.4: Comparison of temperature and stress development calculated with Matlab and PPB during the first 14 days for mix 3.

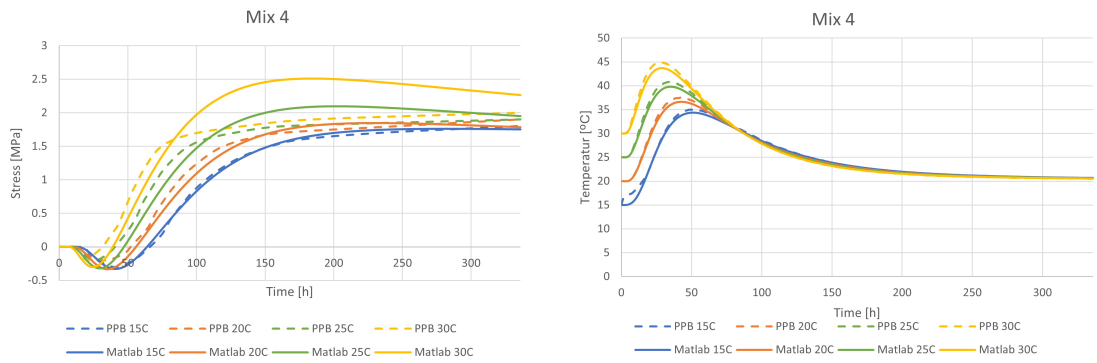

Figure 3.5: Comparison of temperature and stress development calculated with Matlab and PPB during the first 14 days for mix 4.

The temperature development corresponds well with each other, except that PPB reaches a slightly higher maximum temperature. This could also be disregarded since it is the tensile stresses that impact cracking and is of interest for this thesis.

Regarding the stress development, the two models deviate more. The difference between the two models was prominent in the very early stage when the concrete was in compression and as the concrete reaches its capacity. The Matlab model reaches a higher stress than the PPB model as the curve flattens out, this is due to the fact that PPB does not allow for the internal stress to exceed the capacity. PPB uses a non-linear stress-strain behavior when $\sigma/f_{ct} > \alpha_{ct}$, where α_{ct} is a material parameter evaluated by material testing by TCG (Nilsson et al., n.d.). Since it is the actual stress within the concrete that is of interest for this study, the stress was modeled so that its development was calculated independently of the strength and so that the non-linear behavior was disregarded.

One major difference between the two models, is how the viscoelastic behavior was modeled. As mentioned in subsection 3.1.1, PPB uses the real relaxation spectra while the matlab model uses a double power law method with adjustment parameters fitted to the case where the initial temperature equals to 15°C, which could be the reason for the "off-set" between PPB and Matlab in higher initial temperatures. The model captures the phenomenon of stress development correctly and since the study focuses on how material parameters impact stress development and not when or how cracks actually appear, the implemented model was deemed sufficient to be used in the parametric study.

As a part of the model verification, the results of heat and stress/strength ratio was extracted with the purpose to investigate the impact of slag content without no varying of input data. To be able to draw meaningful conclusions about the impact of slag content on certain results, it would be crucial to investigate a larger amount concrete mixes that what was done in this project to be able to see how the results converge relative to the slag content. However, it was considered interesting to investigate this correlation even if the amount of mixes was few, mainly to state the correlation between the values of the input data and the behavior shown in the results from the validation.

3.4 One Factor at the Time analysis

One factor at the time (OFaT) analysis implies varying one input parameter each iteration while keeping all other parameters unchanged. This in order to isolate the impact each parameter has on the development of temperature, stress and strength. The analysis was performed by varying the material input parameters numerically with 20% increase and decrease, in 5% steps, with the data presented in Table 3.2 used as reference values. Altogether the analysis of heat development and stress/strength ratio was performed eight times per parameter and for the the reference combination. Accordingly, 177 analyses were done per mix which made it possible to find a correlation between how much a certain variation of a parameter impacted the heat development and the stress/strength ratio.

3.5 Monte-Carlo simulation

Monte-Carlo (MC) simulation is a sensitivity analysis used in several different fields of science. Monte Carlo simulation uses randomly generated input values to numerically estimate how uncertainty in the inputs affects the results. The input are often based on the probability distribution of a certain input, called the sample space (Wahnström, 2017). Monte-Carlo simulations was used to identify the sensitivity of each parameter on the results of heat development and stress strength ratio. This is done since it will cover a different sample space than the OFaT analysis, also taking the probability distribution into account. As mentioned, the OFaT analysis only varies the parameters $+/-20\%$ regardless of if it is a realistic variance for that parameter or not.

The MC simulation was performed for 100 000 randomly generated parameter combinations based on the probability distribution of each parameters value. In Table 3.3, the standard deviation, coefficient of variance and type of probability distribution are stated for the 22 parameters. This information was obtained from Berrocal et. al. (2024) and was assumed to also apply for low-clinker concrete. That study based the statistical variance on Krauß (2004) except from the variance for the creep adjustment parameters ϕ, d and p which demanded additional simulations. Lastly, the Monte-Carlo simulations included 20 parameters, excluding h_{conv} and R due to that those are more affected of external parameters rather than the concrete mix itself (Berrocal et al., 2024).

Table 3.3: Standard deviation and type of distribution for the 20 parameters.

Parameter	**Standard deviation**	**Coefficient of variance**	**Distribution**
C_c	4.2	0.01	Normal
W_u	6.5	0.02	Normal
t_1	0.24	0.05	Normal
κ_1	0.033	0.02	Normal
θ_{ref}	210	0.05	Normal
κ_3	0.01	0.02	Lognormal
T_{c0}	5	-	Uniform
t_s	0.9	0.15	Lognormal
s	0.015	0.045	Normal
$n_{cc,28d}$	0.025	0.05	Normal
$f_{ct,28d}$	0.22	0.065	Lognormal
β_1	0.067	0.1	Normal
$E_{c,28d}$	2.01	0.06	Lognormal
η_E	0.033	0.1	Normal
ϵ_{su}	34.2	0.25	Lognormal
η_{SH}	0.03	0.1	Normal
ϕ	0.154	0.075	Lognormal
d	0.035	0.075	Normal
p	0.018	0.075	Lognormal
α_T	4e-7	0.04	Lognormal

4

Results

The results from the One Factor at the Time analysis and Monte Carlo simulation are presented in this chapter to visualize the impact and sensitivity of each investigated material parameter, respectively. The chapter is divided into two parts, one for each kind of analysis and presents the results for each mix. Lastly, a summary of the results is included in order to draw conclusions.

4.1 One Factor at the Time analysis

The results from the OFaT analysis are visualized in two different types of plots. The first is a regression plot of how each parameters variance changes the results. The other kind of results are tornado plots stating the impact of each parameter as a number in descending order. In the following sections, the results from the OFaT analysis are presented for all mixes.

4.1.1 MIX 1 reference

First, in order to clearly visualize how the OFaT analysis work, the +/- 20 % variation in three arbitrary parameters and the way it impacted the results was plotted. The parameters chosen were the binder content (C_c), heat of hydration (W_u) and elastic modulus ($E_{c,28d}$). The impact their variance had on heat and stress is plotted in Figure 4.1. As displayed in the figure, the elastic modulus has clear impact on the stress development whereas the change in heat is none. The other two parameters has significant impact on both heat and stress development.

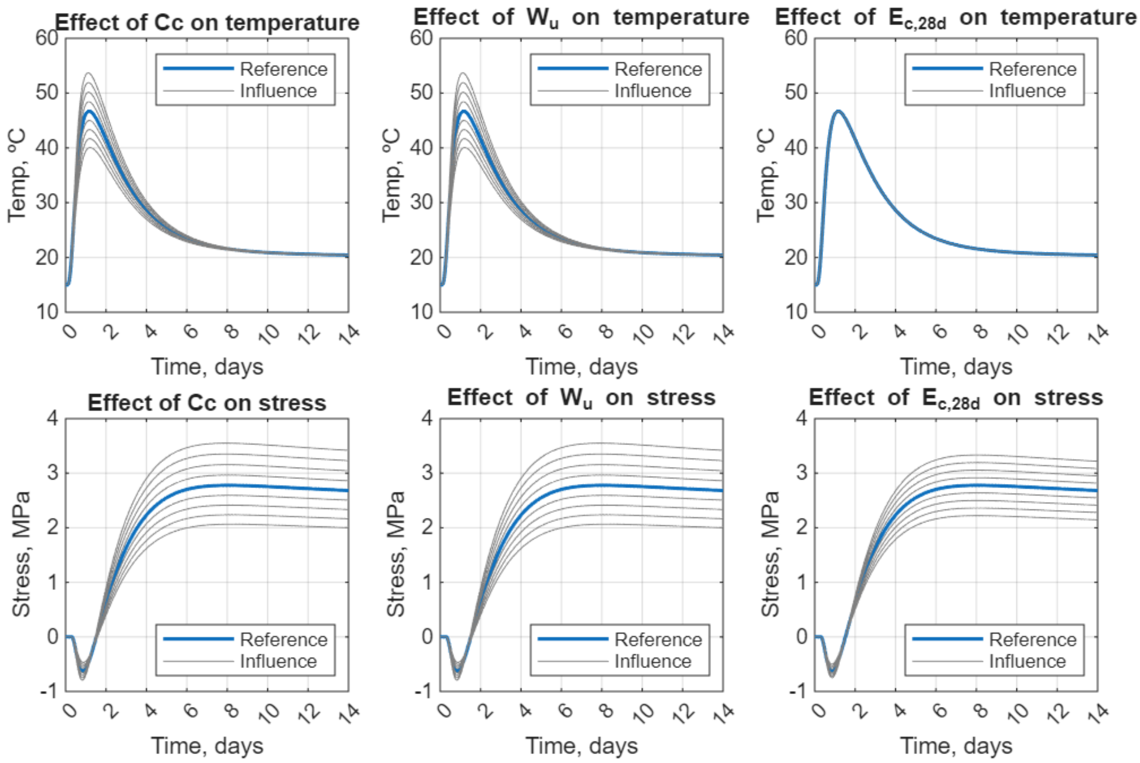

Figure 4.1: Influence of binder content, heat of hydration and elastic modulus on heat and stress development for the reference mix (MIX 1).

The main result from the OFaT analysis was a regression plot. This kind of plot showed the influence of all 22 parameters and how much a certain change of one parameter affected the final result of heat and stress/strength ratio. This result for mix 1 is shown in Figure 4.2. In each subplot, the horizontal axis describes the change of the parameter and the vertical one describes change in final heat and stress/strength ratio. Accordingly, the steeper the slope of the linear regression, the greater the impact that parameter has on the results. A negative slope corresponds that increasing the value of the parameter would decrease the final results, and vice versa.

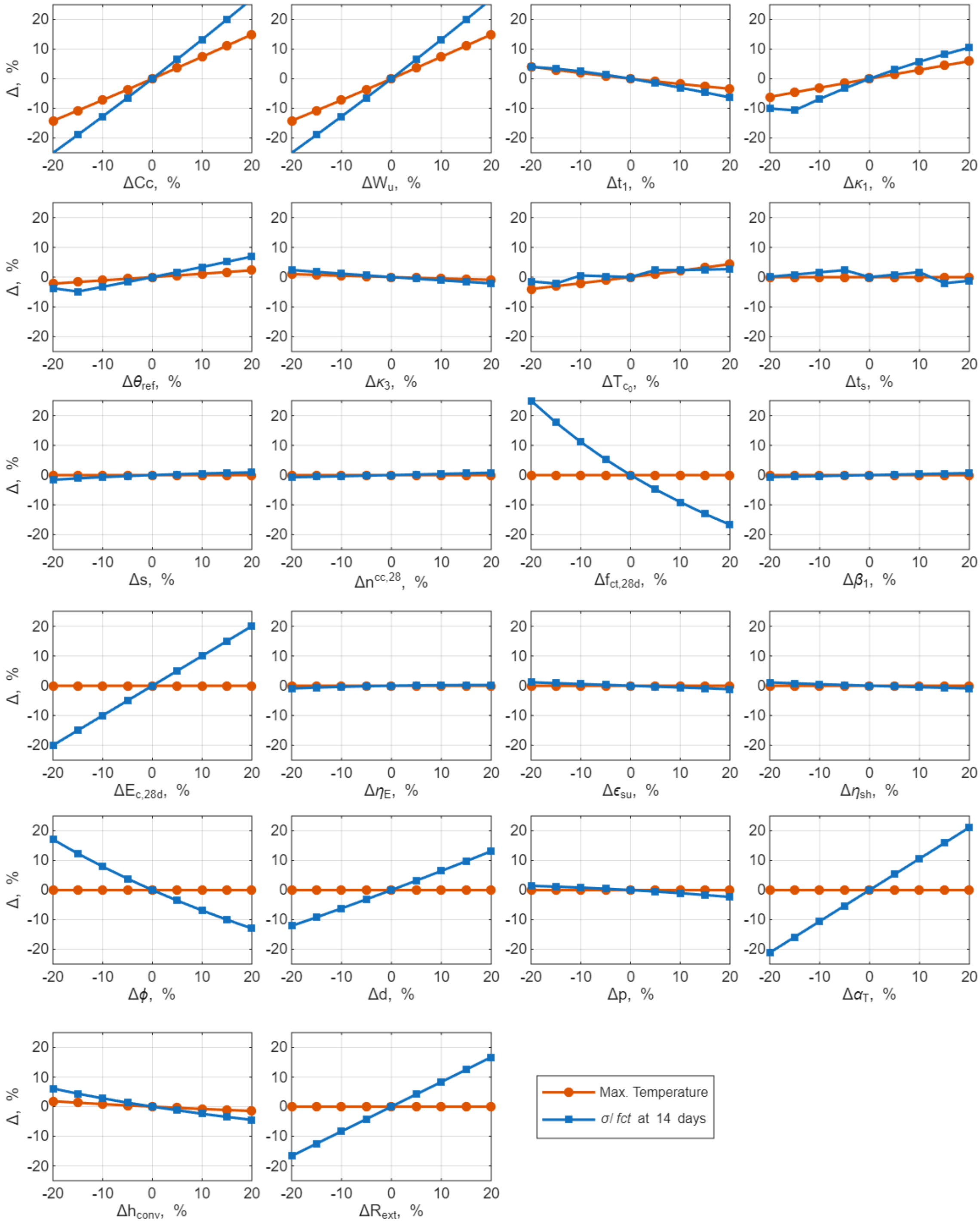

Figure 4.2: Influence of +/- 5%, 10%, 15%, 20% change of every parameter for the reference mix (MIX 1). The blue graphs represents the stress/strength ratio and the red graphs represents the maximum heat developed.

Figure 4.2 shows how certain parameters had great impact on heat and stress ratio, such as binder content (C_c) and hydration heat (W_u), whereas other parameters did not influence the results a lot, for example the adjustment parameters p and $n_{cc,28d}$. Other parameters showed to influence one out of the two results, for example the tensile strength ($f_{ct,28d}$), the external restraint (R_{ext}) and the elastic modulus ($E_{c,28d}$)

had great impact on the stress ratio but none on the heat development, as expected.

The other kind of results was tornado plots showing the impact of each parameter on heat and stress-to-strength ratio stated as a number. The number corresponded to the slope of the regression plot, meaning that the higher the number, the greater the impact. These results are shown in Figure 4.3 and Figure 4.4.

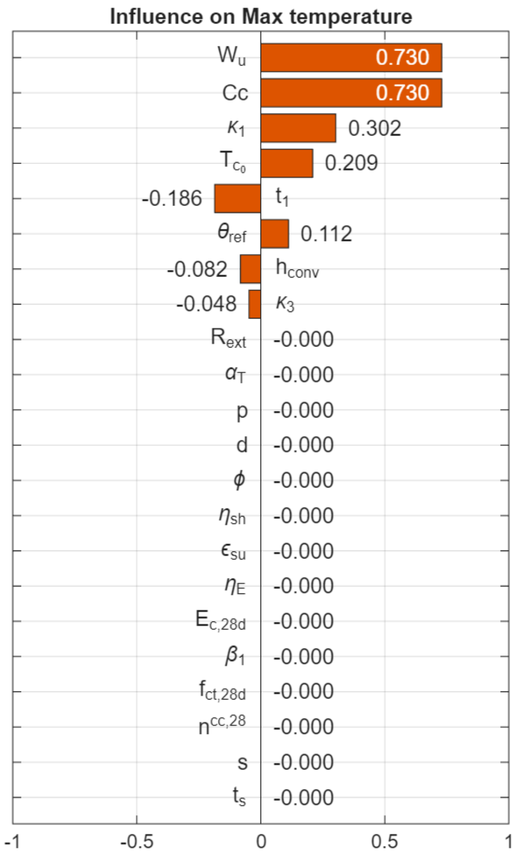

Figure 4.3: Parameter influence on heat development in descending order.

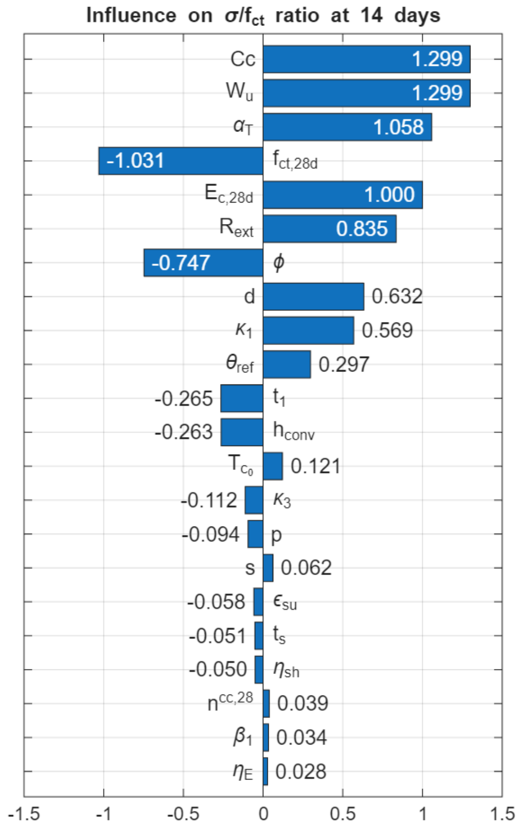

Figure 4.4: Parameter influence on stress/strength in descending order.

Figure 4.3 and Figure 4.4 further indicated that binder content (C_c) and hydration heat (W_u) are the two parameters with the most significant impact on heat and stress ratio. Figure 4.3 and Figure 4.4 also show how more than half of the parameters did not influence the heat development, which is expected since they are not part of the thermal analysis. However, all the parameters influenced the stress ratio to some extent which makes sense studying the constitutive relation in subsection 3.1.1.

4.1.2 MIX 2 16% slag

Mix 2 contained 16% slag and the results from the OFaT analysis for that mix are presented in Figure 4.5, Figure 4.6 and Figure 4.7 following the principle as for mix 1.

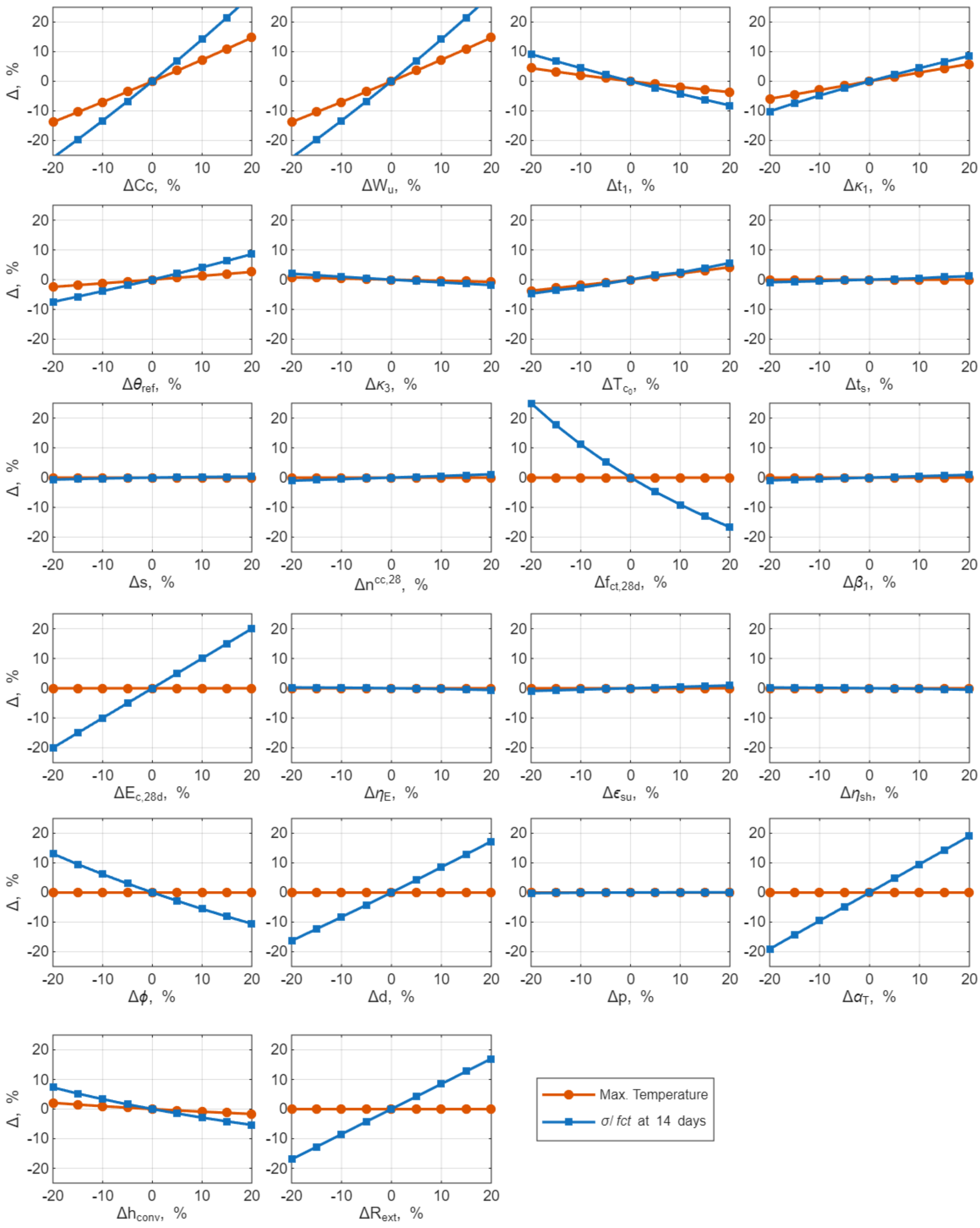

Figure 4.5: Influence of +/- 5%, 10%, 15%, 20% change of every parameter.

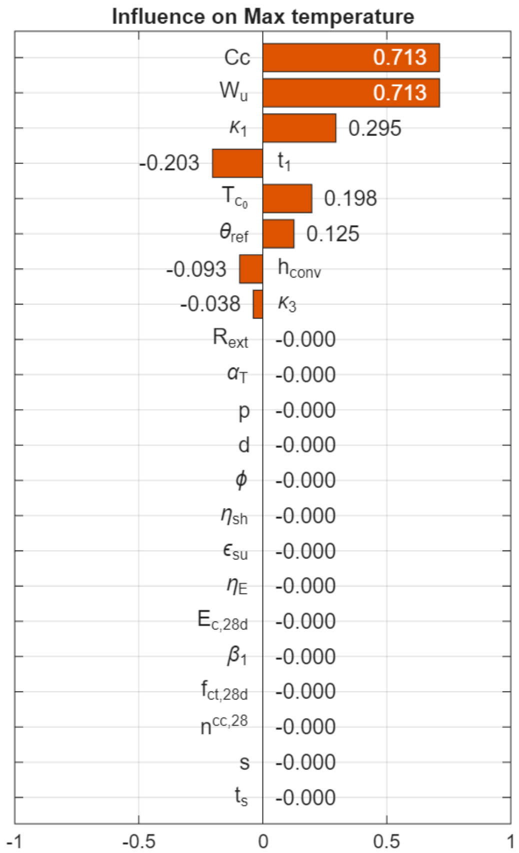

Figure 4.6: Parameter influence on heat development in descending order.

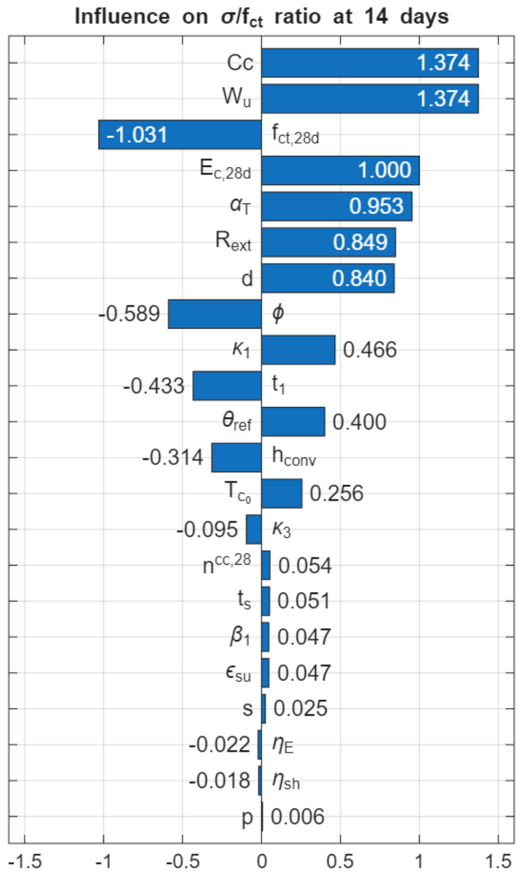

Figure 4.7: Parameter influence on stress-to-strength ratio in descending order.

Directly comparing Figure 4.5 to the corresponding Figure 4.2 for mix 1, the graphs showed similar results. This was further emphasized in the tornado plots which showed the same top three parameters regarding heat development. However, for the stress ratio, the tensile strength showed a more significant impact for mix 2 as it attained the third most significant parameter. This differed from mix 1 where the thermal expansion (and contraction) coefficient (α_T) showed to be the third most significant one.

4.1.3 MIX 3 32% slag

This section presents the results for mix 3, containing 32% slag. The results are presented in the same way as for the previous mixes and are visualized in Figure 4.8, Figure 4.9 and Figure 4.10.

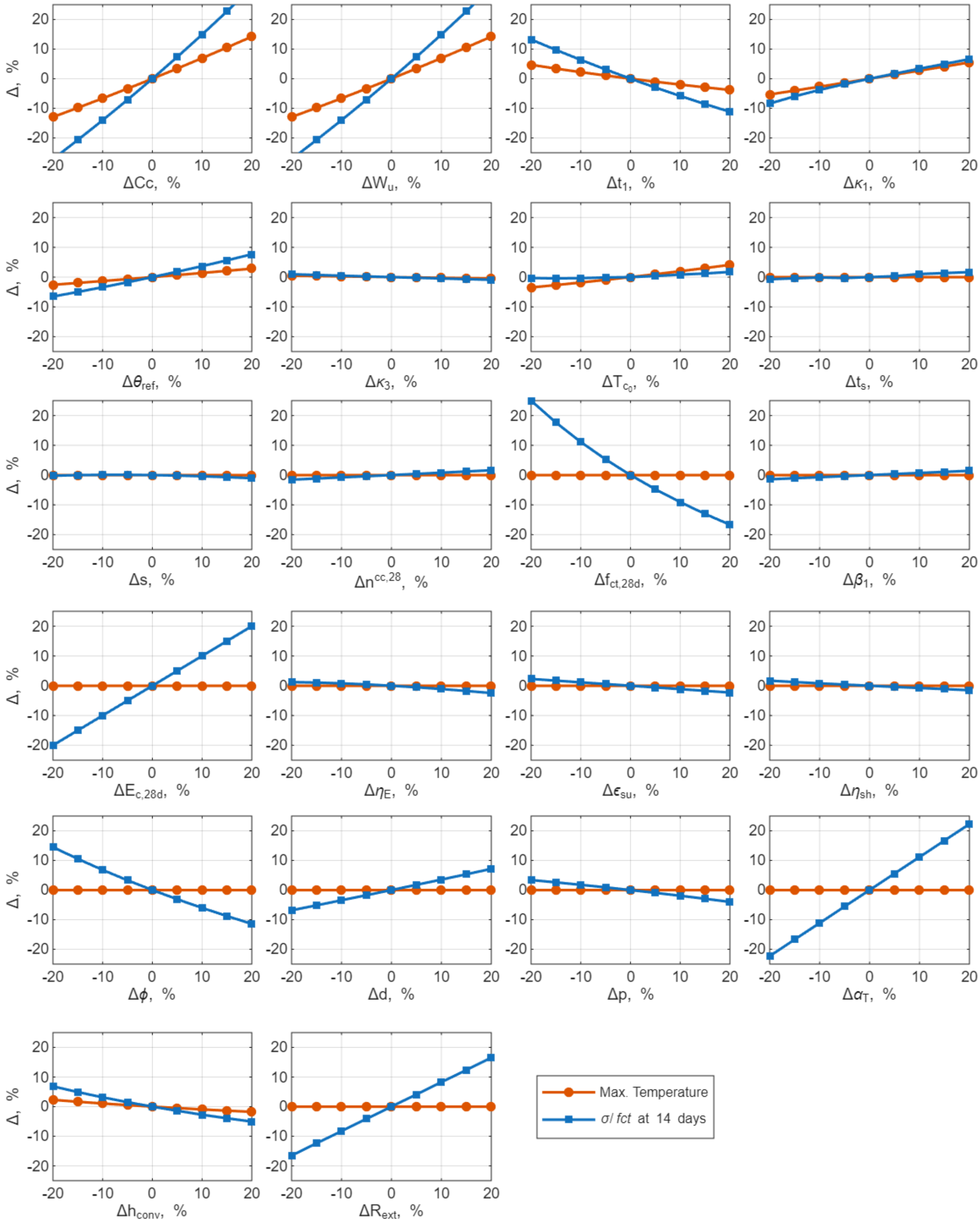

Figure 4.8: Influence of +/- 5%, 10%, 15%, 20% change of every parameter.

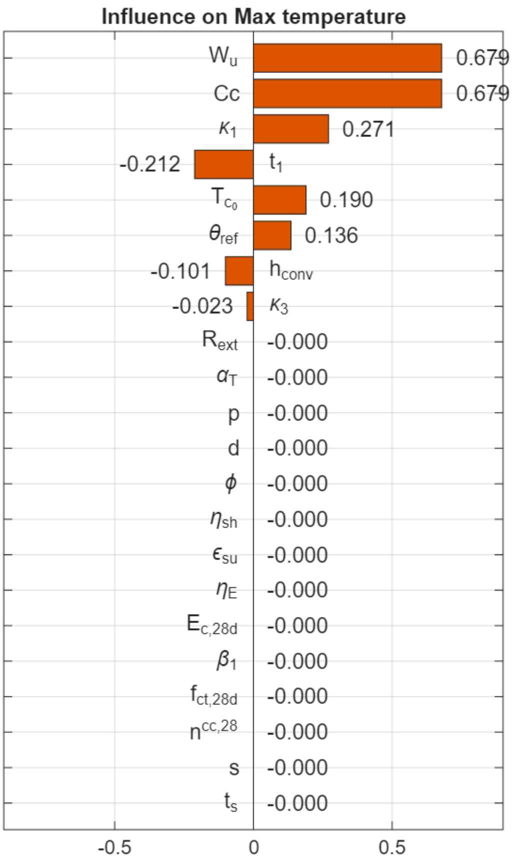

Figure 4.9: Parameter influence on heat development in descending order.

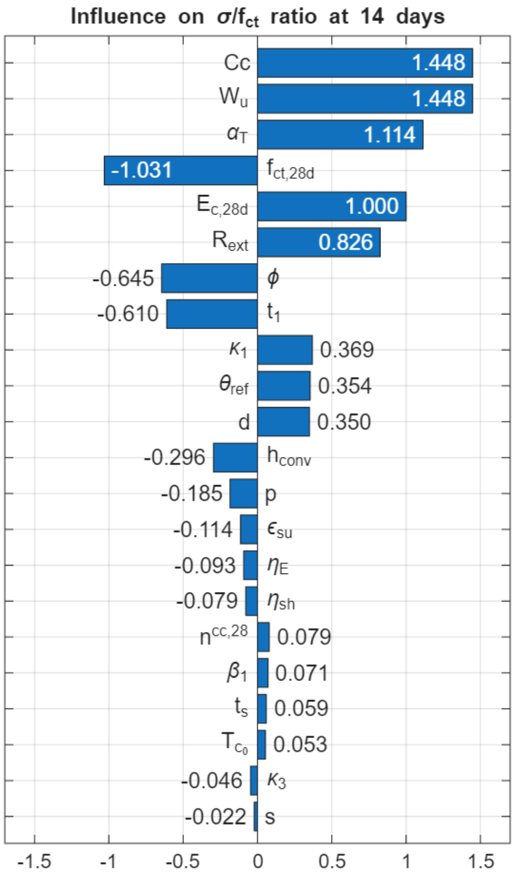

Figure 4.10: Parameter influence on stress-to-strength ratio in descending order.

The results for mix 3 showed regression plots with similar layout as the previous mixes. Analyzing the tornado plots in Figure 4.9 and Figure 4.10, the top three parameters are the same as for mix 1 regarding both heat and stress ratio.

4.1.4 MIX 4 50% slag

The final mix studied in this thesis was one with 50% slag as part of the binder. The OFaT results for mix 4 are presented in Figure 4.11, Figure 4.12 and Figure 4.13, and attained the same layout as for the previous mixes.

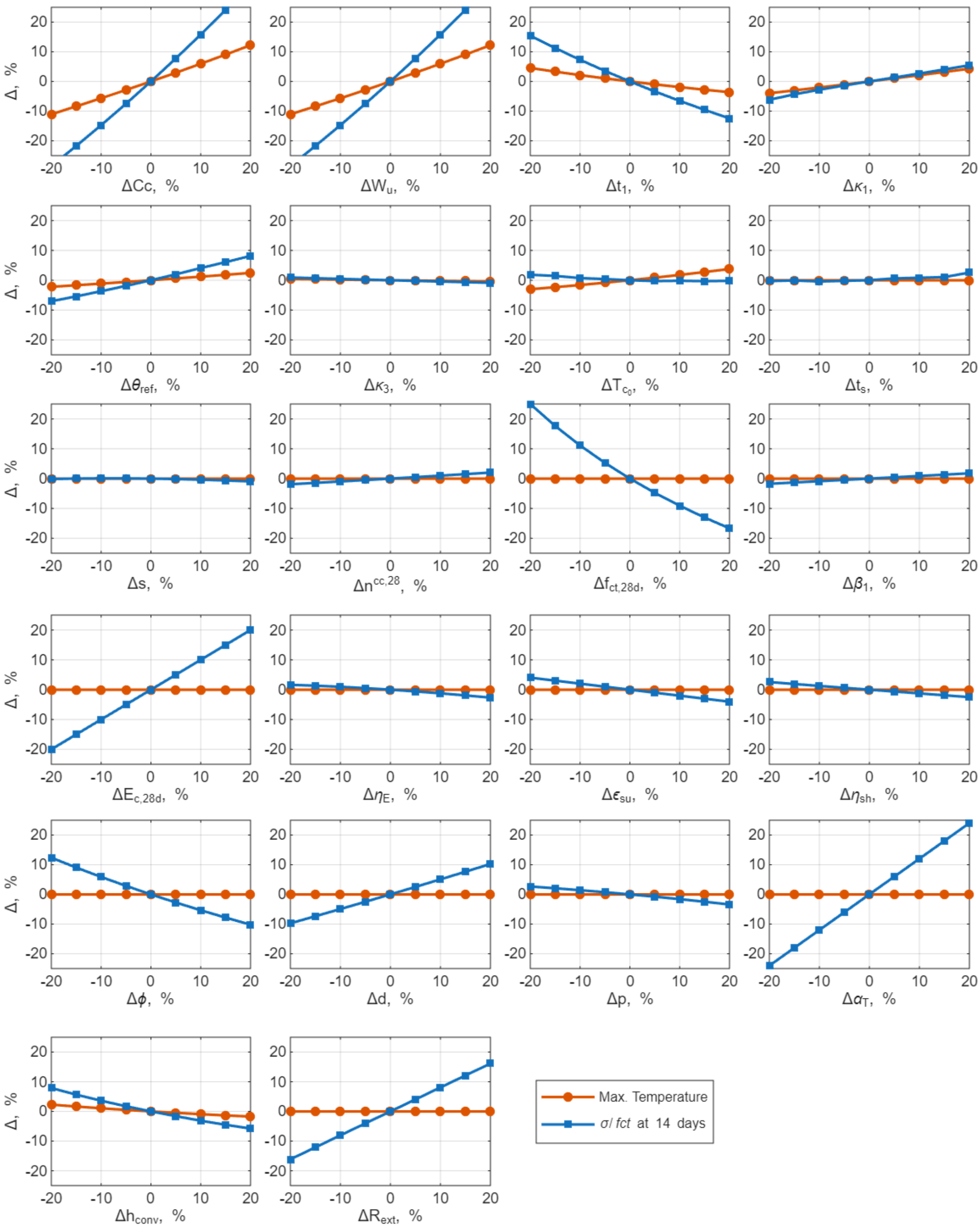

Figure 4.11: Influence of +/- 5%, 10%, 15%, 20% change of every parameter.

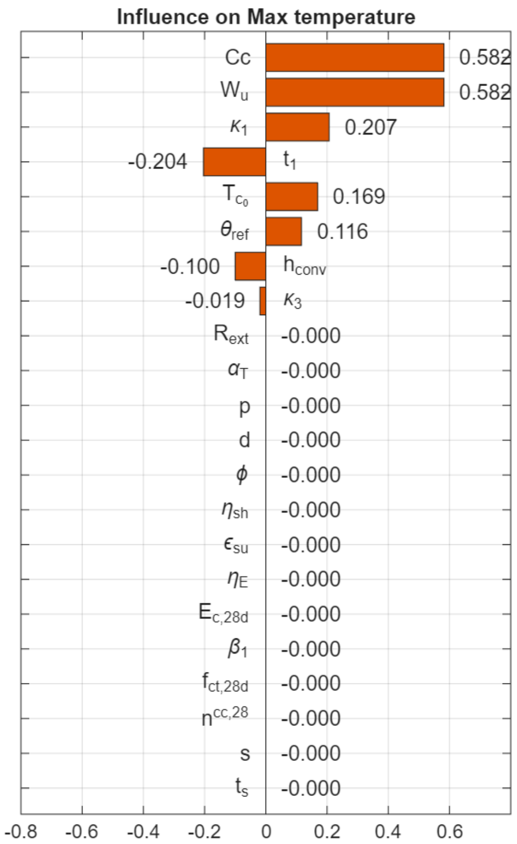

Figure 4.12: Parameter influence on heat development in descending order.

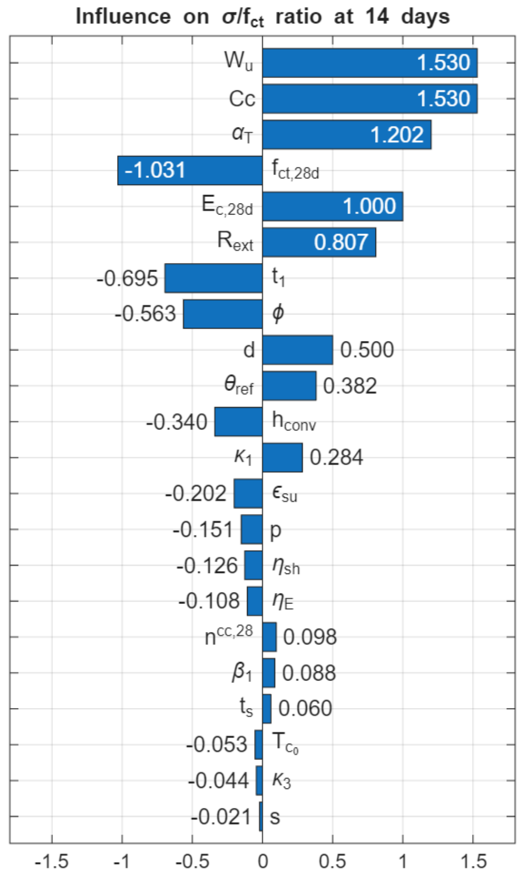

Figure 4.13: Parameter influence on stress-to-strength ratio in descending order.

Figure 4.12 and Figure 4.13 displayed the same top three parameters for both heat and stress ratio as for mix 1 and 3. Furthermore, the tornado plots for all four mixes shared the common feature where the impact of binder content and hydration heat on stress-to-strength ratio was of the exact same magnitude in the OFaT analysis, although the value differed between the mixes.

4.2 Monte-Carlo simulation

The results from the Monte-Carlo simulations are visualized in density plots also containing a linear regression marked in red. The density plots shows the impact on maximum heat and stress-to-strength ratio for the certain change of each parameter obtained within the 100 000 different mix combinations. The combinations were randomly generated based on the statistical data in Table 3.3. Tornado plots were made in addition, visualizing the slope of the regression and accordingly presenting each parameters impact in descending order. This section states the results from the Monte Carlo simulation for the different mixes.

4.2.1 MIX 1 reference

Mix 1 was the reference mix, containing only PC as the binder. The density plots for maximum and stress-to-strength ratio are shown in Figure 4.14 and Figure 4.15 respectively.

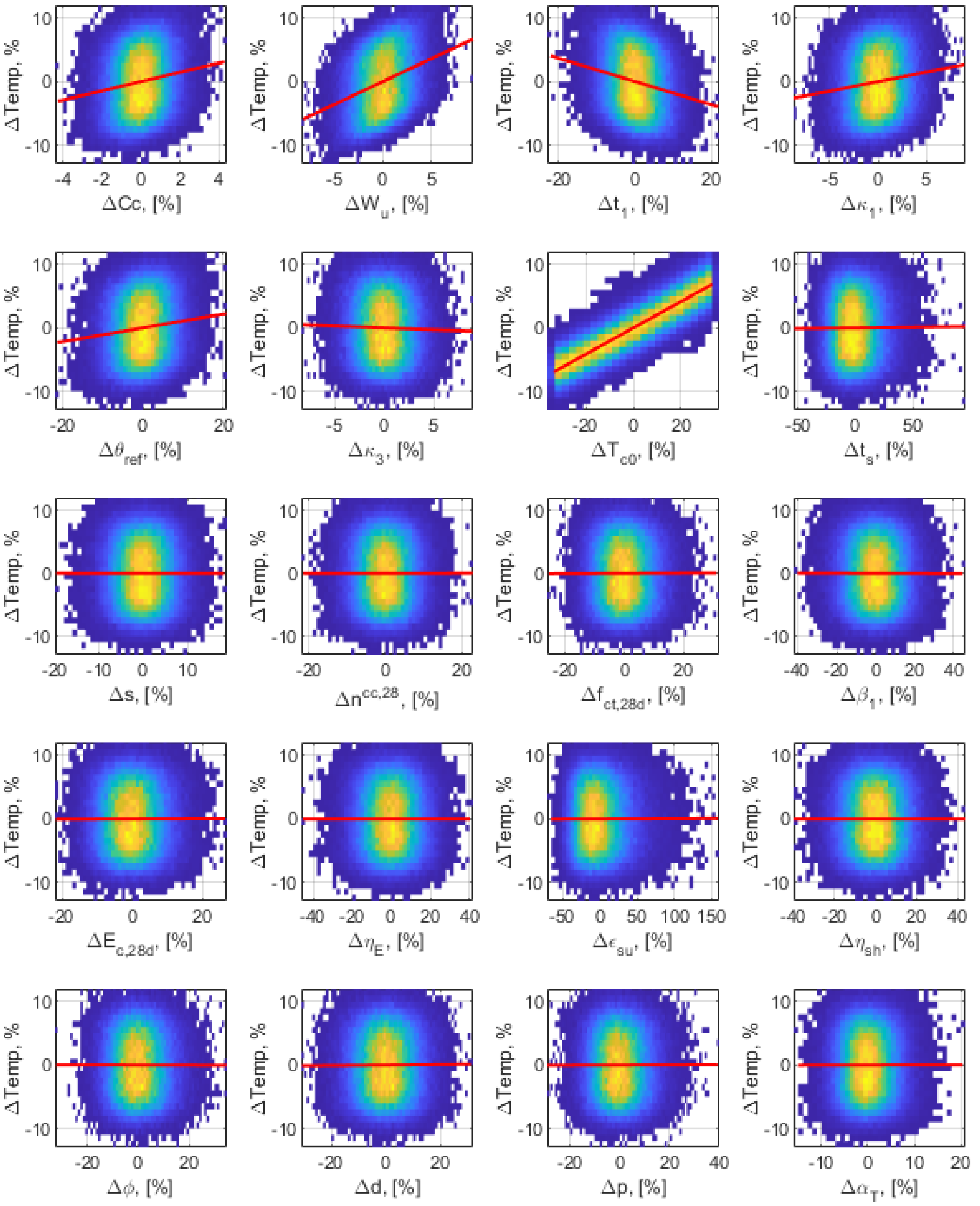

Figure 4.14: Impact on maximum temperature for all parameters with probability based input values (MIX 1).

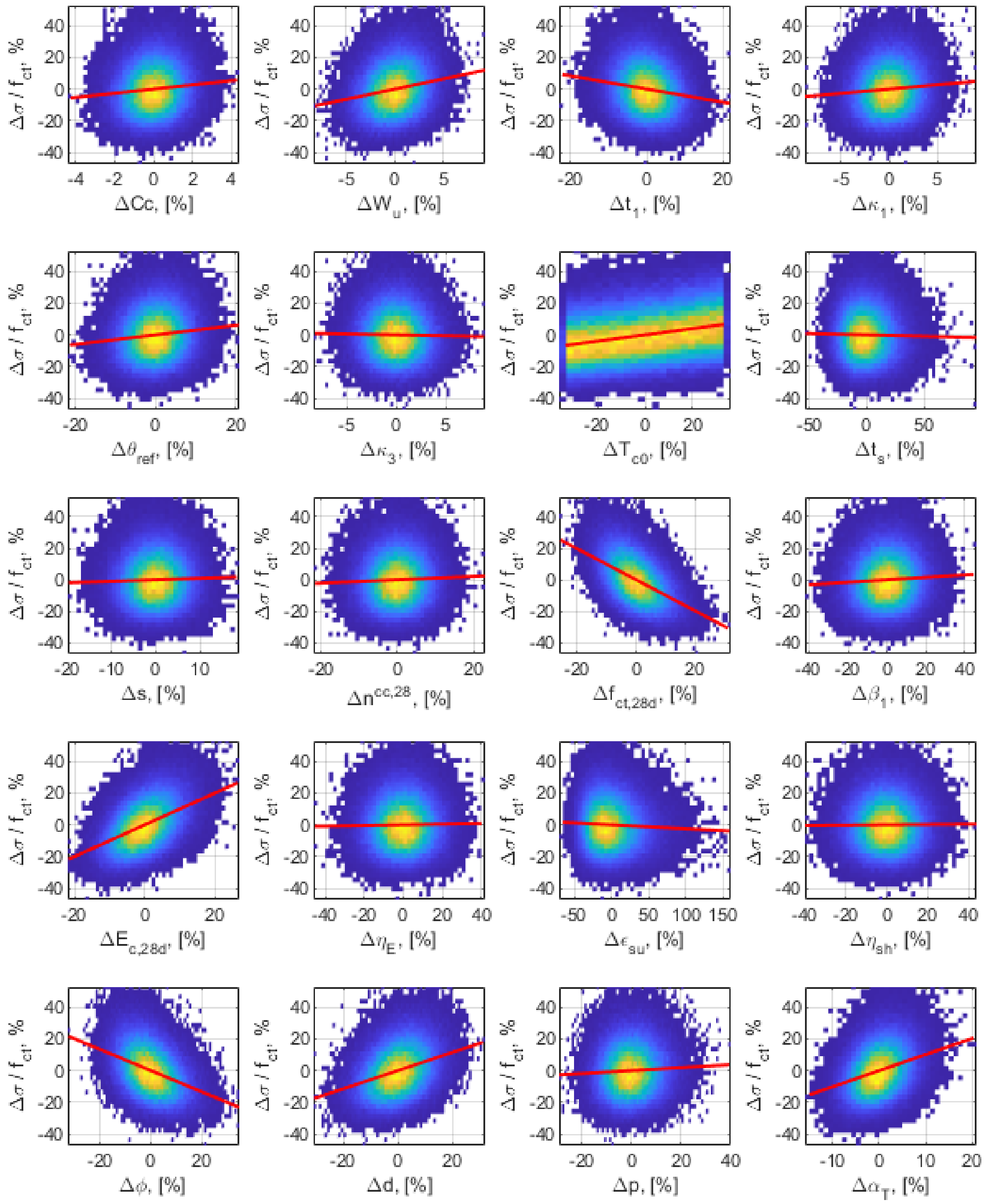

Figure 4.15: Impact on stress-to-strength ratio of every parameter for the reference mix (MIX 1).

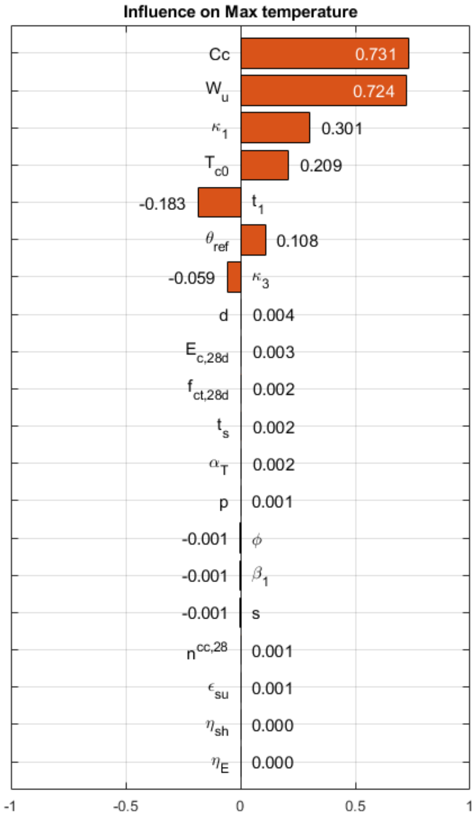

Figure 4.16: Parameter influence on heat development in descending order.

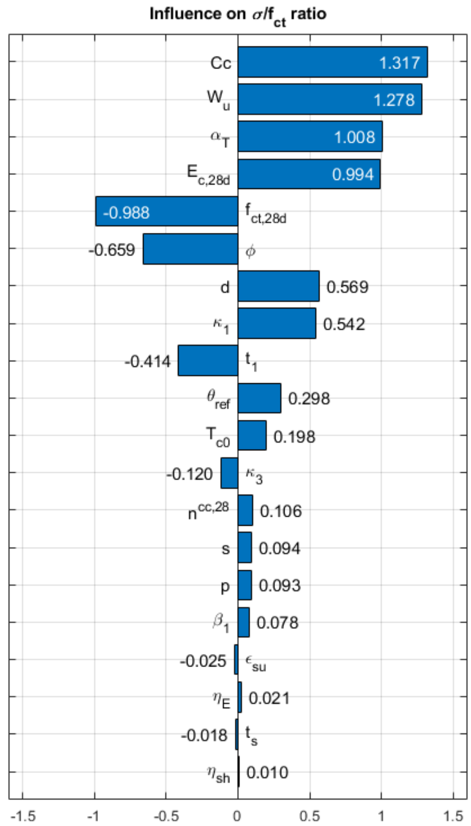

Figure 4.17: Parameter influence on stress-to-strength ratio in descending order.

The slope of linear regression in the density plots shows the direct impact of each parameter as a number and are presented in descending order as tornado plots in Figure 4.16 and Figure 4.17. As for the OFaT analysis, the Monte Carlo simulation showed great impact for the binder content and the heat hydration for both maximum heat and stress ratio. In fact, the top three parameters were the same for mix 1 in both the OFaT and the Monte Carlo simulation.

4.2.2 MIX 2 16% slag

Mix 2 contains 16% slag and the results from the Monte Carlo simulation for that mix are shown in Figure 4.18, Figure 4.19, Figure 4.20 and Figure 4.21.

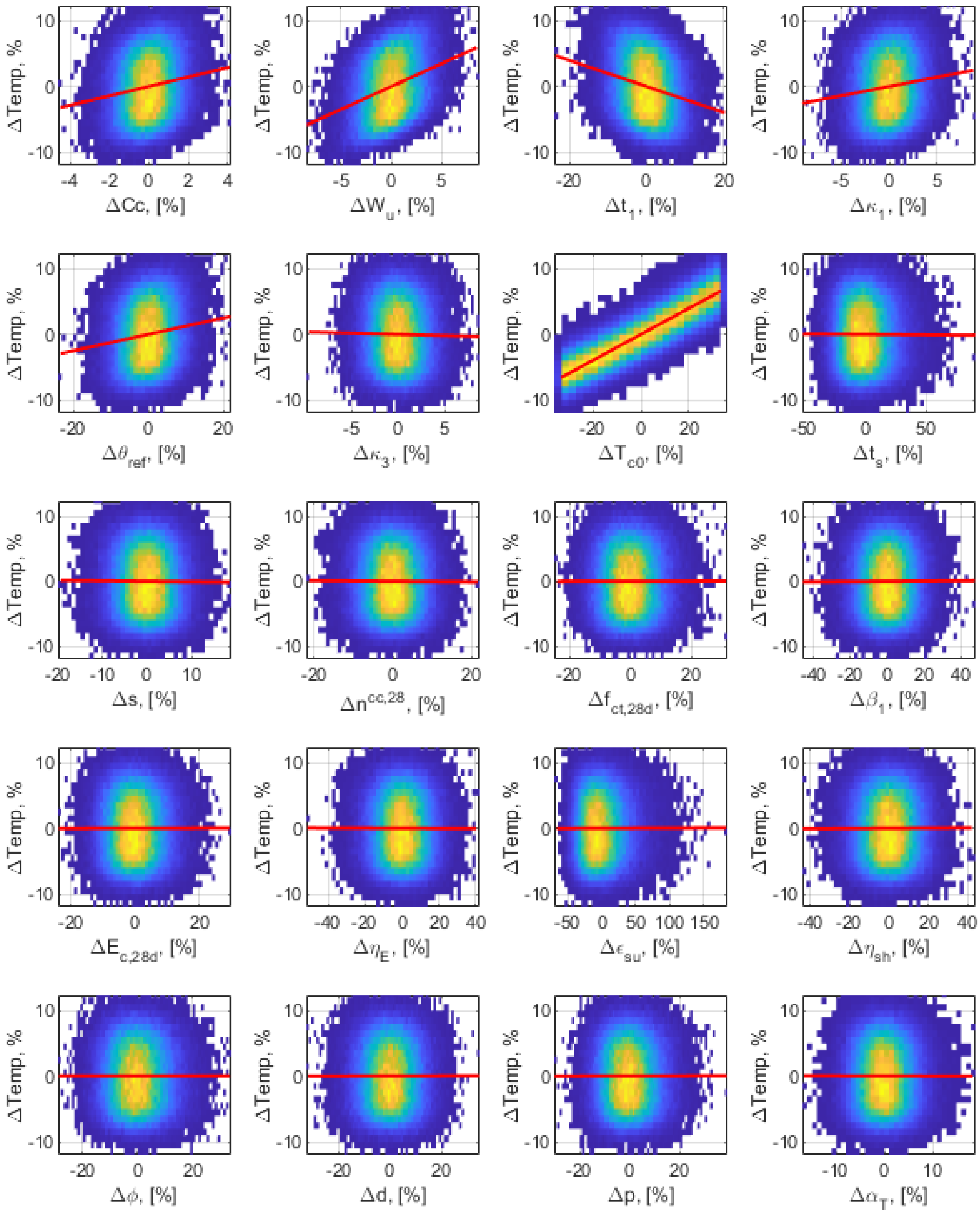

Figure 4.18: Impact on maximum temperature for all parameters with probability based input values (MIX 2).

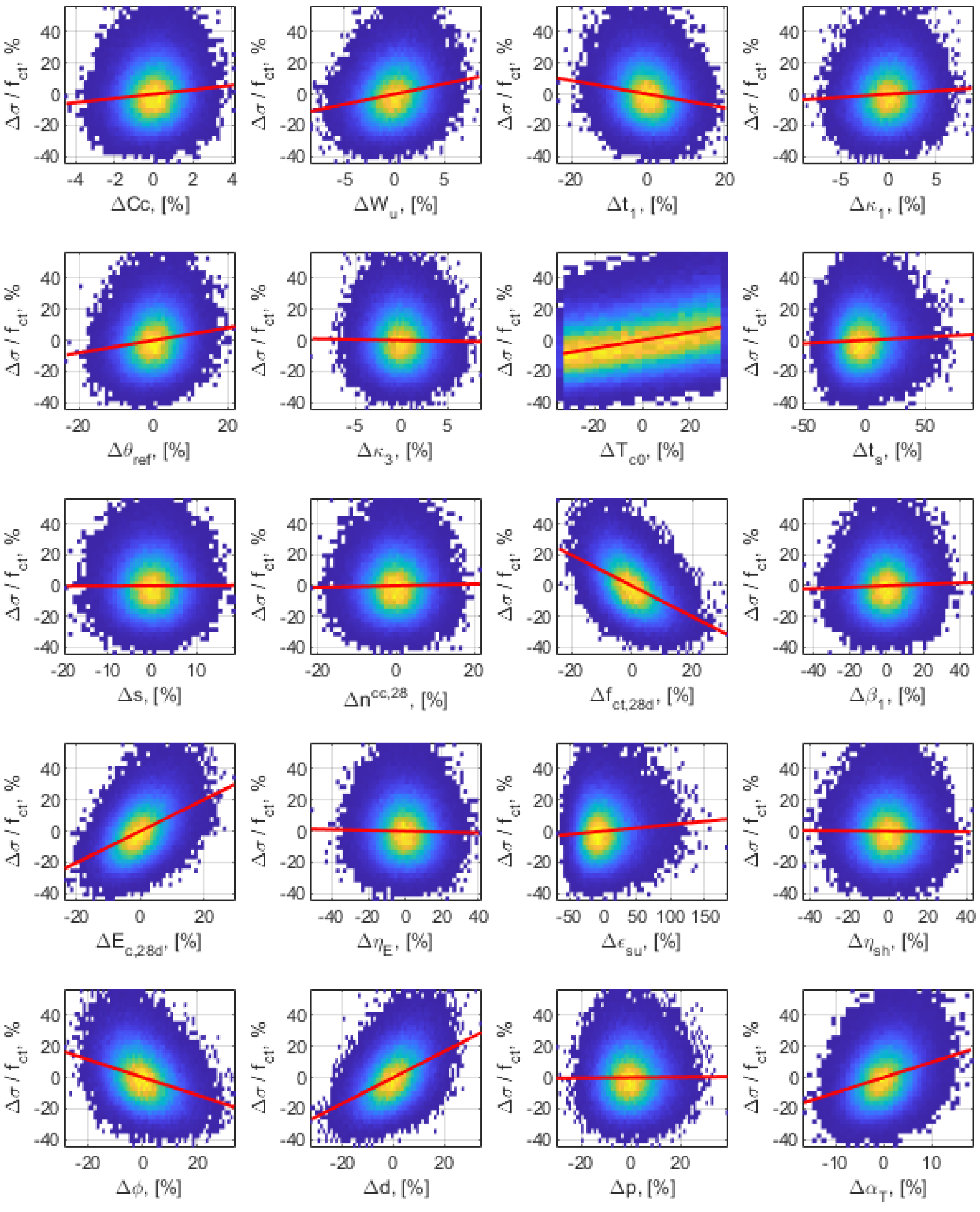

Figure 4.19: Impact on stress-to-strength ratio of every parameter for the reference mix (MIX 2).

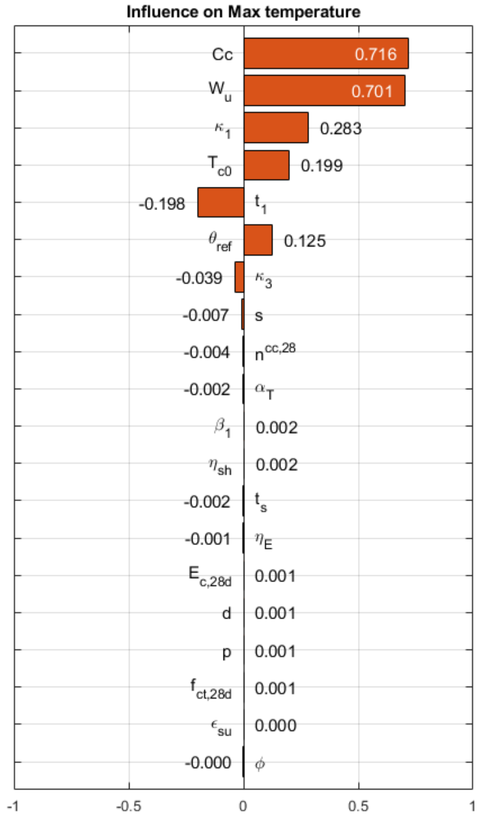

Figure 4.20: Parameter influence on heat development in descending order.

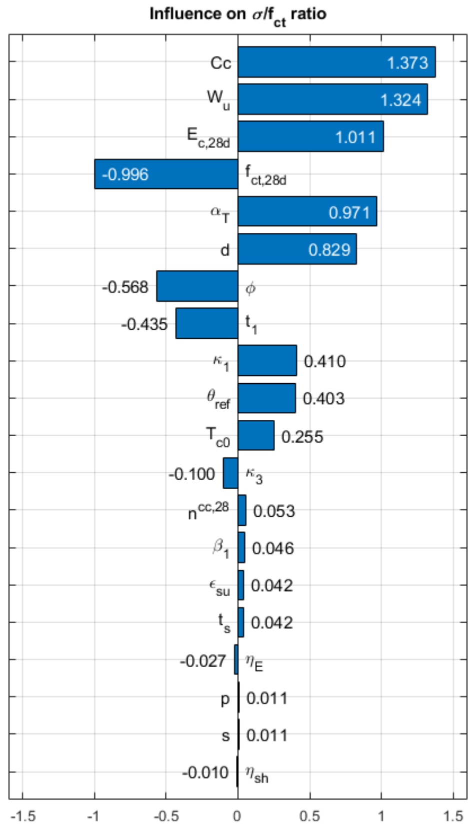

Figure 4.21: Parameter influence on stress-to-strength ratio in descending order.

Similar to the corresponding results from OFaT-analysis, the ranking of most influential parameters differs slightly between Mix 1 and Mix 2. The coefficient of thermal expansion is ranked lower, though it still demonstrates a significant impact on the stress-to-strength ratio.

4.2.3 MIX 3 32% slag

Mix 3 contains 32% slag and the results from the Monte Carlo simulation for that mix are shown in Figure 4.22, Figure 4.23, Figure 4.24 and Figure 4.25.

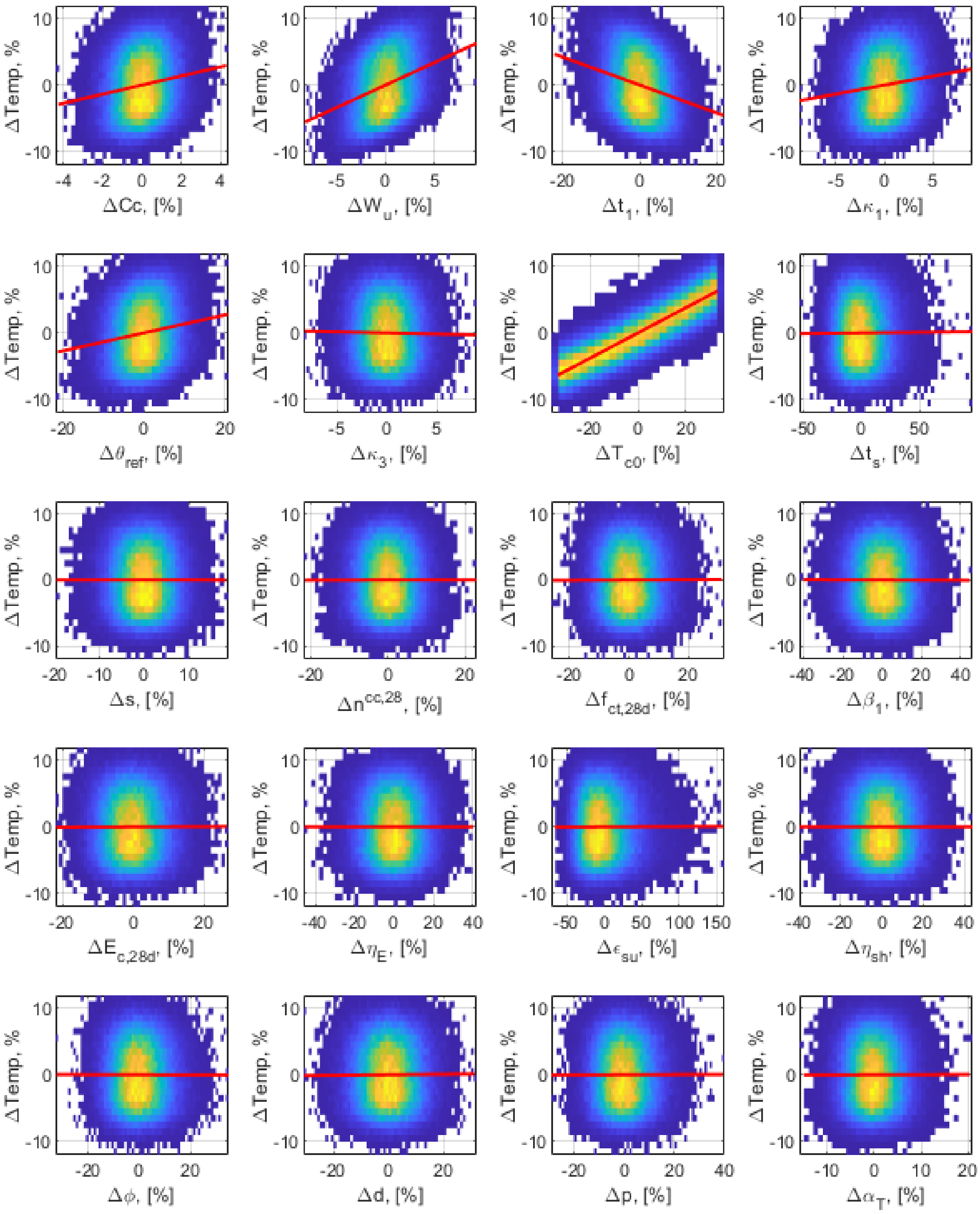

Figure 4.22: Impact on maximum temperature for all parameters with probability based input values (MIX 3).

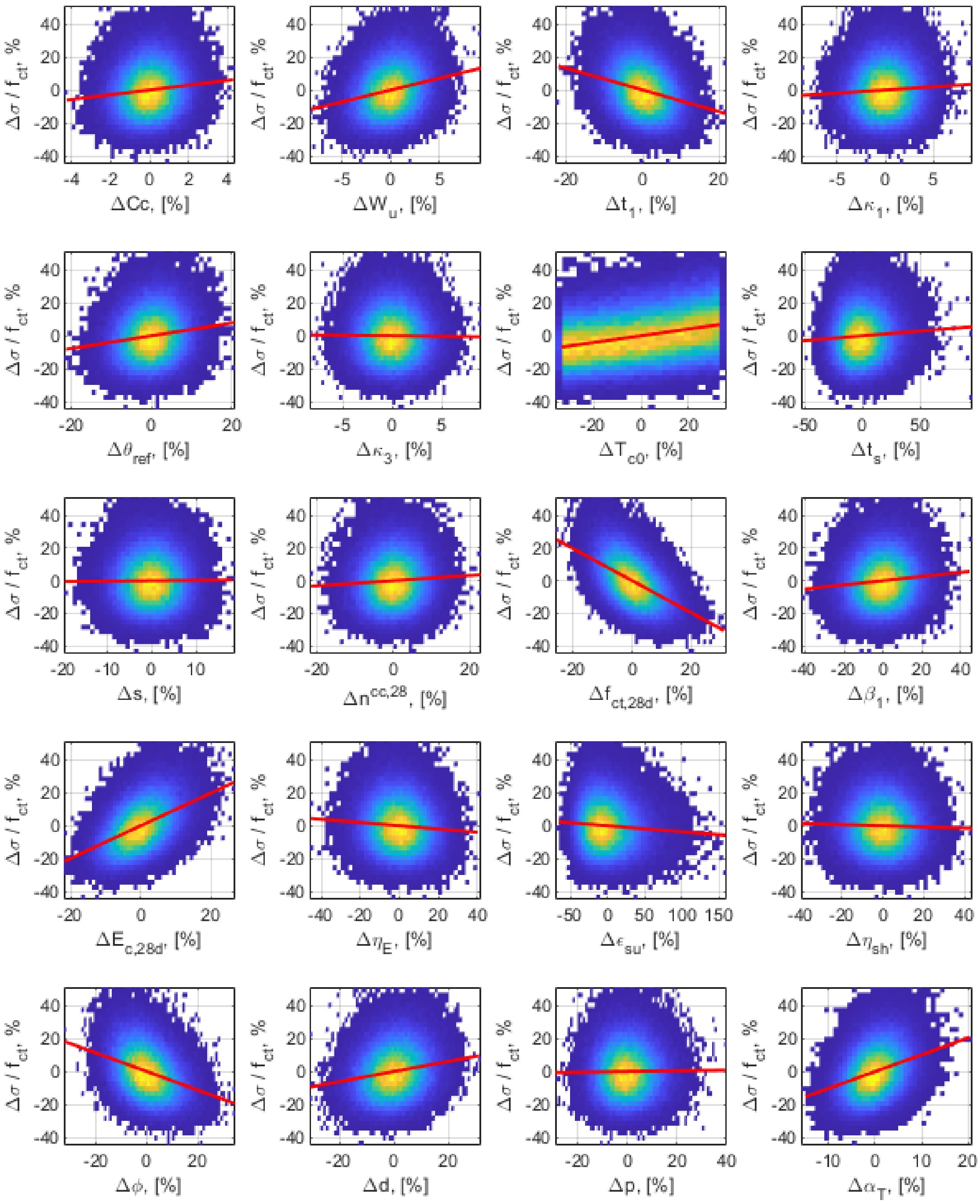

Figure 4.23: Impact on stress-to-strength ratio of every parameter for the reference mix (MIX 3).

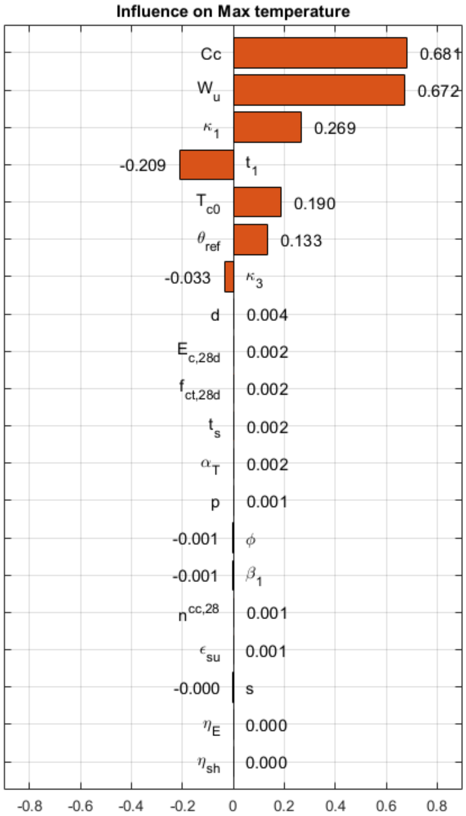

Figure 4.24: Parameter influence on heat development in descending order.

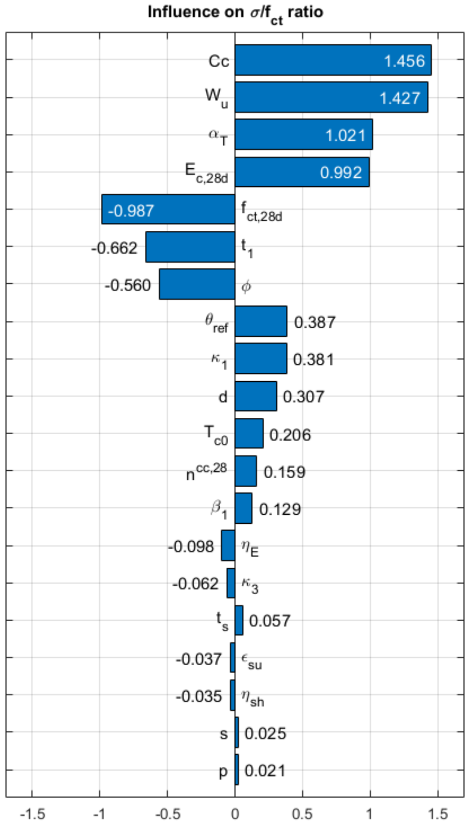

Figure 4.25: Parameter influence on stress-to-strength ratio in descending order.

The Monte Carlo simulation for mix 3 shows the same top parameters as for mix 1, and further indicates that the binder content, heat of hydration and thermal expansion are three parameters with great impact on thermal cracking. In addition, the top parameters are the same for mix 3 in both the OFaT analysis and the Monte Carlo simulation.

4.2.4 MIX 4 50% slag

Mix 4 was the concrete with slag as half of the binder content. The results from the Monte Carlo simulation for mix 4 are presented in Figure 4.26, Figure 4.27, Figure 4.28 and Figure 4.29.

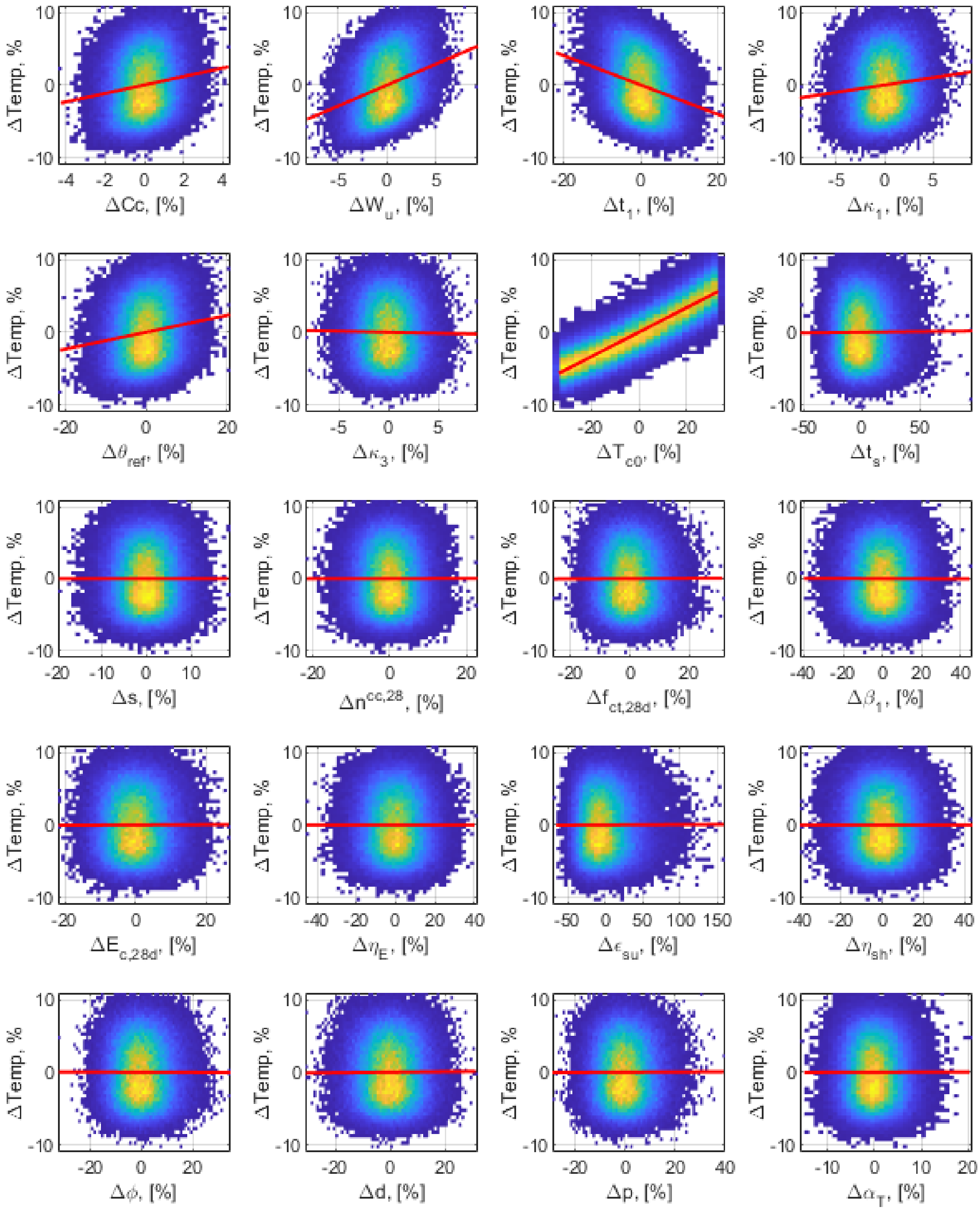

Figure 4.26: Impact on maximum temperature for all parameters with probability based input values (MIX 4).

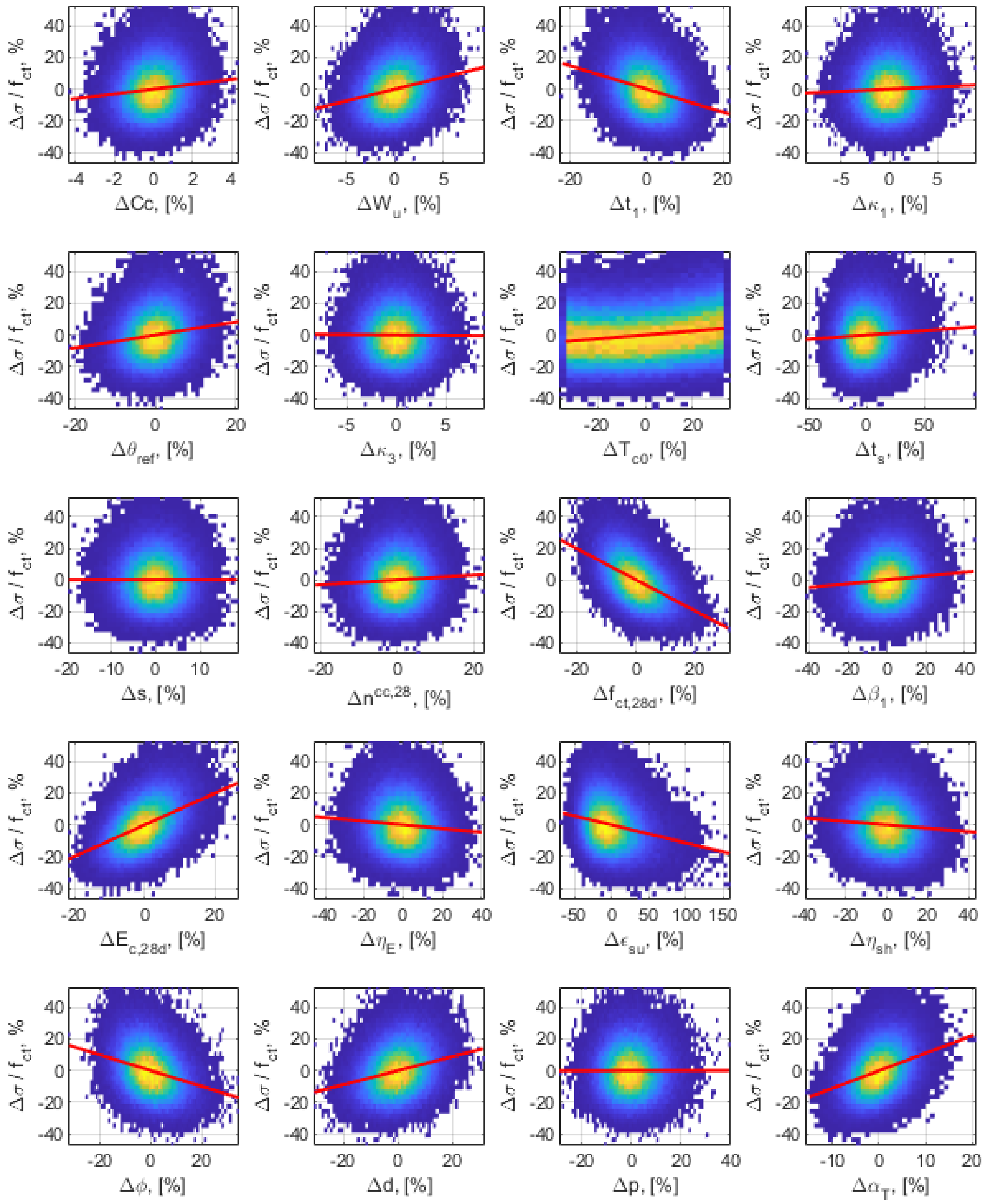

Figure 4.27: Impact on stress-to-strength ratio of every parameter for the reference mix (MIX 4).

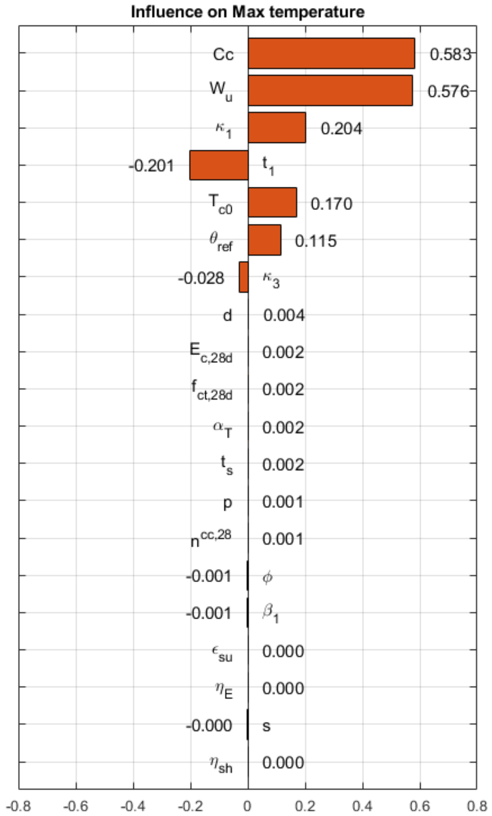

Figure 4.28: Parameter influence on heat development in descending order.

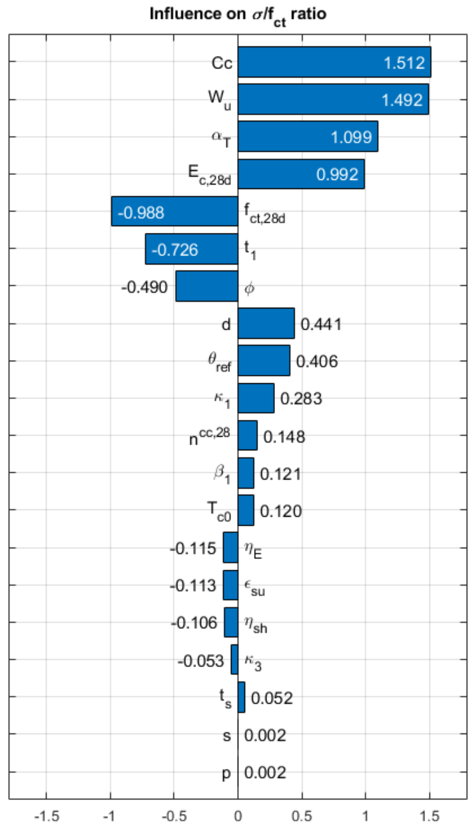

Figure 4.29: Parameter influence on stress-to-strength ratio in descending order.

The results from the Monte Carlo simulation for mix 4 shows the same top three parameters as for mix 1 and 3, both Monte Carlo and OFaT. Although the parameters with the greatest impact are the same across all mixes, the magnitude of their influence is not identical, causing differences in the ranking of the most important parameters between recipes. Nevertheless, the differences in influence are relatively small, and the actual impacts remain of a similar magnitude across all parameters and recipes.

5

Discussion

In this chapter, the results from the OFaT analysis and Monte Carlo simulation will be independently assessed but also compared to each other. The parameter ranking will be discussed and compared to previous parametric studies made on concrete with OPC. The assumptions made, the model and its limitations will also be discussed.

5.1 Model setup and assumptions

The results indicate that there is a clear correlation between slag content and heat development. As expected, higher content of OPC leads to increased maximum temperature and increased thermal stresses. The model produces a realistic thermal and structural response and the assumption that the same equations could be used for low-clinker concrete and regular concrete could be deemed accurate. Since the material parameters are tested for a specific concrete mixture, the behavior of slag is reflected in the material properties, for instance that the final heat of hydration decreases with increasing slag content. Accordingly, the assumption made was considered relevant.

5.2 OFaT-analysis

The OFaT analysis showed that parameters directly associated with the hydration process had the largest influence on heat development. The final heat of hydration (W_u) and the binder content (C_c) were the most influential parameters on the maximum temperature. This is consistent with the governing equations, where both parameters directly determine the total amount of heat generated during the hydration. These two parameters are closely linked to each other and based on the heat development equations, increasing or decreasing either one of the parameters result in an equally large change in temperature, which then is reflected in the stress-to-strength ratio as well. This explains why the impact of those parameters are of the same magnitude for all four mixes in the OFaT analysis.

Apart from binder content and heat of hydration, the parameters κ_1, t_1 and T_{c0}, which control the rate and timing of the temperature development and at which time maximum temperature occurs, are among the top most influential parameters. Since the heat development is such a fundamental part of stress development one may expect the top five most crucial parameters in the temperature development to correspond to the most important parameter for stress. This is however not the case, even though κ_1, t_1 and T_{c0} have large impact on the temperature, the connection to stress and strength development is only secondary leading to lower ranking.

Continuing on the stress-to-strength ratio, W_u and C_c remain most significant. The tensile strength ($f_{ct,28d}$), modulus of elasticity ($E_{c,28d}$) and external restraint (R_{ext}) are also of great importance together with the thermal expansion coefficient, α_T. Thermal strains are directly transformed into stresses under restrained conditions. Increasing α_T increased the magnitude of thermal deformation and consequently produced larger tensile stresses during cooling. Interestingly enough, the thermal expansion is one of the parameters not measured in Sweden. It is adjusted to fit the measured total autogenous and thermal deformation obtained in testing. To actually evaluate this parameter would be time consuming and complicated, but evidently of great importance.

The impact of change of $f_{ct,28d}$ and $E_{c,28d}$ on the stress-to-strength ratio is large but it is also the exact same despite the varying of slag content, which is visualized in Figure 5.1. We can interpret this as concrete being generally sensitive to a change of these two parameters, but in this type of OFaT analysis, not dependent on the concrete composition. The equations describing the development of tensile strength and stress are functions of the 28-day tensile strength and elastic modulus, respectively, as well as the content of slag. Calculating the ratio of stress and strength essentially eliminates the material dependent part of the equation. Basically, the sensitivity of these two parameters to the stress-to-strength ratio is independent of recipe. However, since the two parameters still have a large impact on the stress-to-strength ratio, they are important to measure for a certain concrete mix in order to perform a reliable cracking analysis.

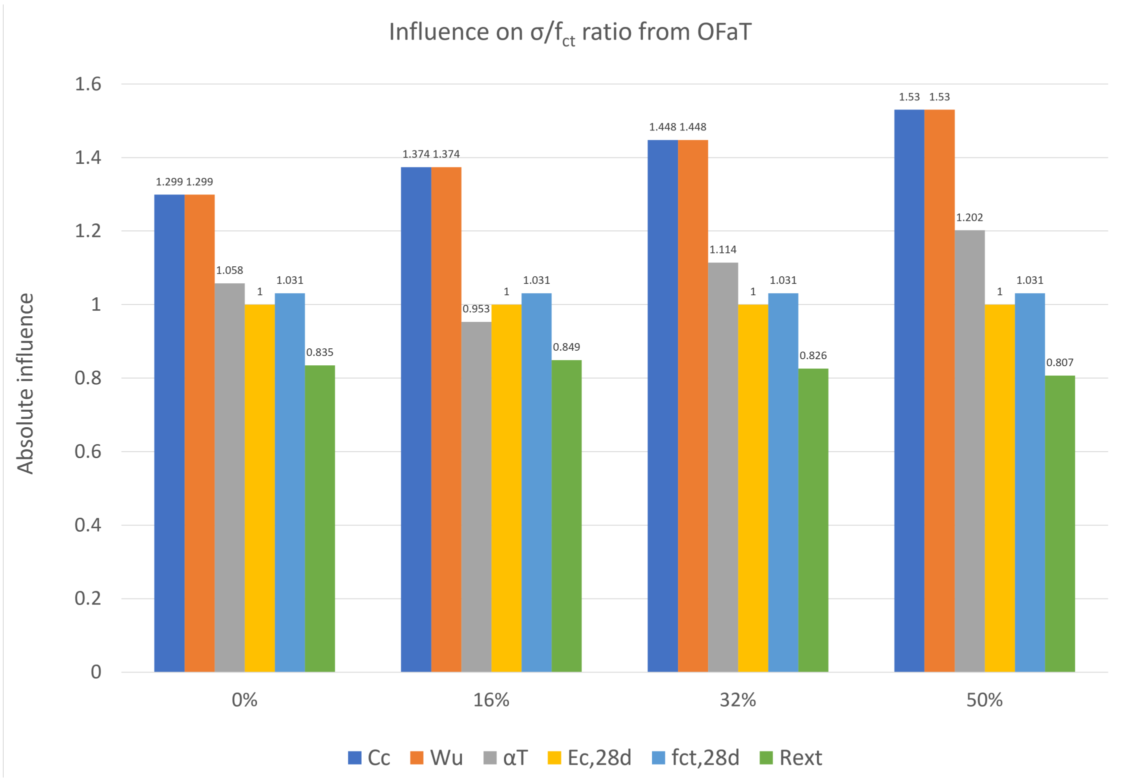

Figure 5.1: Absolute influence of binder content, heat of hydration, thermal expansion coefficient, modulus of elasticity, tensile strength and external restraint for all four concrete mixes.

The ranking of the top five most important parameters are relatively consistent between all mixes. The only difference in the ranking of importance is in mix 2 where the thermal expansion coefficient is in placement five instead of three. This can be linked back to the input data where mix 2 had the lowest thermal expansion coefficient of all mixes. Furthermore, this parameter is obtained by adjustments to fit the measured deformation rather than measured directly, which introduces uncertainties to the input data.

Further studying the OFaT analysis, a certain amount of parameters showed no impact on the thermal development for all mixes. This is expected since those are not a part of the constitutive relation for heat development, see subsection 3.1.1. However, all parameters impact the stress-to-strength ratio to some extent, although some of which are small. As mentioned previously, the method of OFaT is inherently flawed in the regards that the analysis disregards the interaction between parameters and therefore a more comprehensive sensitivity analysis was needed, which is why a Monte Carlo simulation was preformed.

5.3 Monte Carlo

The Monte Carlo simulation bases the randomly generated parameters on their probability distribution and the relationship between the different parameters, both of which have to be known. Monte Carlo provides more realistic cases for the analyses, where several parameters change simultaneously rather than independently. The Monte Carlo simulations provide an insight to the sensitivity of each parameter in a context which aims to be statistically realistic.

The tornado plots show that the risk of early-age thermal cracking is controlled by a limited number of dominant parameters, while the majority have negligible influence. The sensitivity analysis validates that the binder content and the heat of hydration are dominant factors influencing both the maximum temperature and the stress-to-strength ratio. Both factors contribute to the heat released during the hardening of the concrete. Higher cement content means more reactive material during the hydration process, while increased hydration heat translates to more energy released per unit of cement. Higher temperatures lead to larger thermal gradients and higher stresses within the concrete.

The results also indicate that some material parameters may be negligible which could make the cracking risk assessment and implementation of new concrete recipes more efficient. However, determining which parameters can be considered negligible is not straight forward. The influence of a parameter depends not only on its individual contribution, but also the interaction with other parameters and the specific behavior of the concrete recipe. A parameter with limited influence for one mix may become more important for another mix which makes defining a strict threshold for negligible parameters complicated. But the possibility to identify parameters that consistently show low influence could contribute to more efficient implementation of new low-clinker concrete recipes by prioritizing testing on parameters with the greatest impact on cracking.

5.3.1 Comparison to the OFaT-analysis

The results from OFaT and Monte Carlo are generally in agreement, except for some difference in ranking which is summarized in Table 5.1. This suggests that the interaction between parameters influence the structural response and that the effect of one parameter may depend on the values of others. The Monte Carlo analysis also highlighted that some parameters with limited individual influence in the OFaT analysis became more significant when interacting with other variables. This illustrates the limitations of OFaT analyses, specifically that they neglect parameter interactions and therefore cannot fully capture the complexity of concrete behavior.

Table 5.1: Top five parameters from each analysis for all four mixes.

	OFaT				Monte Carlo			
Ranking	Mix 1	Mix 2	Mix 3	Mix 4	Mix 1	Mix 2	Mix 3	Mix 4
1	C_c/W_u	C_c/W_u	C_c/W_u	C_c/W_u	C_c	C_c	C_c	C_c
2	α_T	$f_{ct,28d}$	α_T	α_T	W_u	W_u	W_u	W_u
3	$f_{ct,28d}$	$E_{c,28d}$	$f_{ct,28d}$	$f_{ct,28d}$	α_T	$E_{c,28d}$	α_T	α_T
4	$E_{c,28d}$	α_T	$E_{c,28d}$	$E_{c,28d}$	$E_{c,28d}$	$f_{ct,28d}$	$E_{c,28d}$	$E_{c,28d}$
5	R_{ext}	R_{ext}	R_{ext}	R_{ext}	$f_{ct,28d}$	α_T	$f_{ct,28d}$	$f_{ct,28d}$

Contrary to the OFaT-anaysis where the regression coefficient for C_c and W_u is the exact same (Figure 5.1), the heat of hydration ranked slightly lower in the Monte Carlo simulation (Figure 5.2). The reason for this could be due to its dual effect of increasing the thermal stresses while also accelerating the strength development so that its overall impact on the stress-to-strength ratio decreased. Despite this compensating mechanism, its overall impact on the risk of early-age cracking remains significant.

5.3.2 Recipe dependency

Similarly to the OFaT analysis, there are trends connected to the slag content that can be analyzed within the result. The trends are visualized in Figure 5.2. For example, the sensitivity to binder content and heat of hydration increases with increasing slag content. One possibility could be that the maximum developed stress is lower for higher amounts of slag. This generates larger sensitivity to the changes made in the parametric analyses, which is why they are calculated as having more impact for mixes with high slag content.

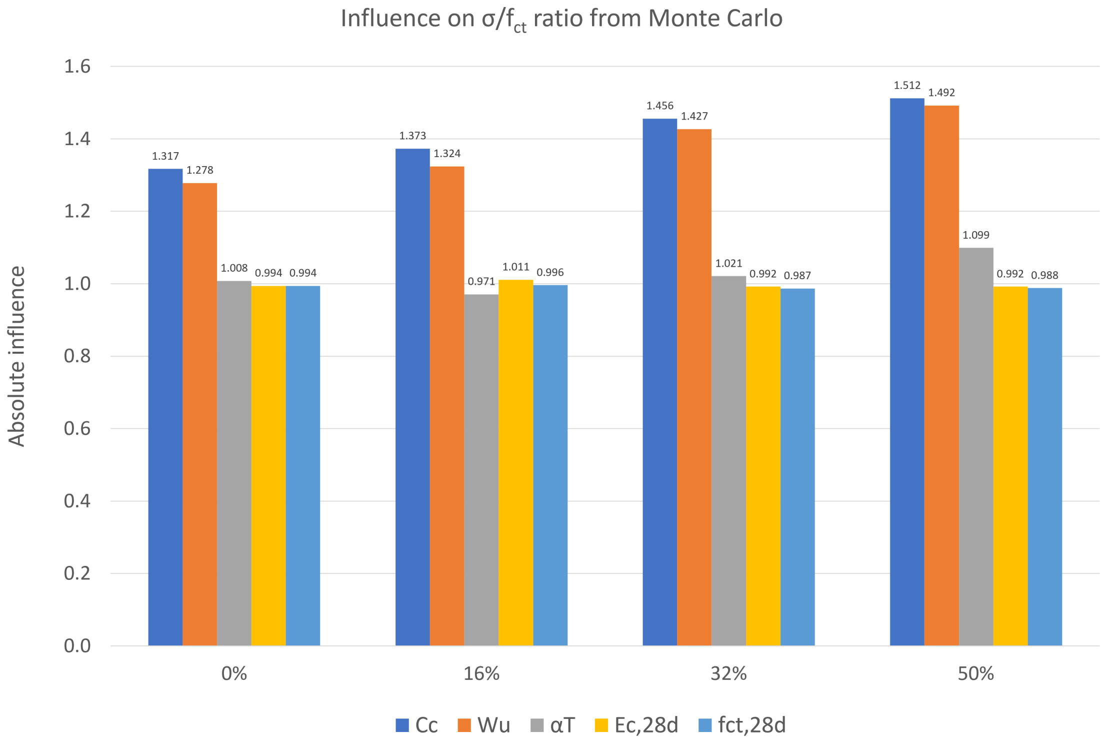

Figure 5.2: Absolute influence of binder content, heat of hydration, thermal expansion coefficient, modulus of elasticity and tensile strength for all four concrete mixes.

The slag content also correlates to the maximum temperature but in the opposite way. The higher the slag content, the lower the impact of the binder content. This is because the slag generates less heat than OPC and therefore, the binder content does not create as drastic change in temperature for the mixes with higher slag content. However, whether or not we can draw any actual conclusion from the sensitivity trends is questionable. It is challenging to directly compare parameter sensitivity between the different concrete recipes. Each recipe was calibrated using its own set of reference parameters in order to simulate its specific material behavior. Consequently, the baseline conditions differed between the mixes before any parameter variations was introduced.

This means that a change in one parameter does not necessarily produce the same physical effect for all recipes, since the response also depends on the remaining adjusted and estimated parameters and the overall behavior of the mix. For example, a variation in a hydration-related parameter may have different consequences depending on the slag content, strength development, creep behavior or thermal response of the specific recipe. As a result, it becomes difficult to establish universal relationships between parameter changes and structural response across all mixes. The observed sensitivity is not only a function of the varied parameter itself, but also of the interaction between that parameter and the reference values of each concrete recipe. The results should therefore primarily be interpreted as recipe specific trends rather than universally applicable sensitivities. Nevertheless, some general tendencies could still be identified. The fact that the ranking of importance agrees between recipes indicates that although the absolute sensitivities differ between mixes, the governing physical mechanisms remain similar.

The response of the model is heavily dependent on the selected reference parameters. Since each concrete recipe requires its own calibrated parameters to produce realistic material behavior, the sensitivity analysis became highly dependent on the quality and accuracy of the input data. This highlights the importance of reliable testing methods for obtaining material parameters used in early-early age crack risk analyses. Small uncertainties in parameters with large impact may significantly affect the predicted stress-to-strength ratio and consequently the estimated cracking risk.

5.4 Comparing concrete mixes

The general trends observed in this study agree well with previous research on low-clinker concrete and early-age thermal cracking, in the sense that slag reduces peak temperature and tends to delay the development of tensile strength.

Table 5.2: Top five parameters from the previous study (Berrocal et al., 2024).

	OFaT	**Monte Carlo**		
Ranking	Regression	Correlation	Regression	Random Forest
1	C_c	$f_{ct,28d}$	C_c	$f_{ct,28d}$
2	W_u	$E_{c,28d}$	W_u	$E_{c,28d}$
3	$f_{ct,28d}$	$T_{c,0}$	$f_{ct,28d}$	$T_{c,0}$
4	$E_{c,28d}$	d	$E_{c,28d}$	d
5	κ_1	ϕ	κ_1	ϕ

Comparing the results from this study, specifically the MC-simulation, to the previous study by Berrocal et. al. (2024), the two parameters with the most influence on thermal cracking for regular concrete are the same as for concrete with SCMs. $f_{ct,28d}$ and $E_{c,28d}$ are both ranked high for low-clinker concrete and concrete with OPC, though different placements. The ranking in the previous study is presented in Table 5.2. The biggest difference is the fact that the adjustment parameter, κ_1, is highly ranked in the previous study, while the thermal expansion coefficient, α_T, ranked higher in this thesis. This could be linked back to the reference parameters used for each mix. The low-clinker mixes generally had a lower κ_1 and a higher α_T. Since some of the initial values differ quite drastically between recipes, it is questionable which values are actually reasonable, highlighting the importance of parameter testing accuracy.

Studying the results regarding heat development, the regression analysis of the Monte Carlo simulation in the previous study showed cement content, heat of hydration, the adjustment parameter κ_1, initial concrete temperature and the maturity adjustment parameter t_1 as the top five. Apart from a difference in order, those are the same as the top five for all mixes studied in this thesis regarding the influence on maximum temperature. One conclusion that can be drawn in connection with this is that SCM has a greater impact on the stress/strength ratio than the heat development.

5.4.1 Model instability

Monte Carlo simulations are more computationally demanding compared to OFaT. The randomly generated parameters occasionally resulted in unrealistic material behavior, causing numerical instability in the model. In these cases the model produced undefined values (NaN = Not a Number), particularly for mix 3 and mix 4, which contained higher slag contents. Approximately 30 parameter combinations had to be removed due to these instabilities before running the simulation. A possible explanation for these numerical issues is that the randomly generated parameters created physically unrealistic combinations of thermal and mechanical properties. Another contributing factor is that the Monte Carlo simulations treated the parameters as statistically independent. In reality, several material properties are physically correlated, such as compressive and tensile strength, E-modulus, creep and shrinkage. Randomly generating parameters without accounting for these correlations may therefore produce combinations that would never occur in reality.

Despite these removed parameter combinations, the Monte Carlo simulations are still considered representative and useful. The excluded parameter sets represented only a very small fraction of the intended 100 000 combinations. Consequently, the statistical distribution and overall trend of the results were not significantly affected. The remaining simulations still provided a sufficiently large sample size to identify parameter sensitivities and variability in structural response.

6
Conclusion

This work aimed to investigate the effect of SCM on the heat development and overall risk for early-age thermal cracking as well as parameter sensitivity in low-clinker concrete. This was investigated numerically through a simplified thermo-mechanical analysis of a 700 mm wide wall slice using two parametric approaches. In this chapter the conclusion of the study will be presented with regards to the initial research questions. Further more, areas for future work will be discussed.

6.1 Conclusions

In conclusion it is possible to state that the parameters with the most impact on thermal cracking in early-age low-clinker concrete are the binder content and the heat of hydration. The study also showed the great impact of the thermal expansion (and contraction) coefficient, tensile strength and the modulus of elasticity. Creep related parameters also showed significant influence while parameters related to shrinkage generally were rated lower.

The parameters with the most impact on thermal cracking are the same for low-clinker and regular concrete, to some extent. As an example, the thermal expansion coefficient, though always showing a significant influence independent of the concrete recipe, ranked different depending on the mix design. It is generally difficult to establish a clear connection between the slag content and what parameter has the most influence on thermal cracking since each mix is defined by individual tests. These parameters are also adjusted or estimated to comply with the testing results which is cause for some uncertainty. The results should therefore primarily be interpreted as recipe specific trends rather than universally applicable sensitivities.

Another important aspect of the study concerns the possibility of simplifying the implementation of new concrete recipes. Since obtaining recipe-specific material parameters requires extensive testing, reducing the number of necessary input parameters could make practical implementation of early-age crack risk analyses more efficient. The sensitivity analyses indicate that some parameters consistently had a relatively small influence on either the temperature development or the stress-to-strength ratio within the investigated parameter intervals. Such parameters could potentially be generalized instead of using recipe-specific values, thereby reducing the required amount of testing for new concrete mixes. However, the threshold for parameter importance is difficult to state. Generally, the parameters related to autogenous shrinkage are rated lower, while parameters related to creep seem to be of more importance.

6.2 Further research

During the project several areas for future work and recommendations were identified. In addition to the linear regression analysis there are other types of analyses to apply to the Monte Carlo simulation. Correlation analysis or machine learning approaches including random forest methods could be applied to better understand parameter importance and parameter interaction. Introducing parameter correlation models or applying bounded probability distributions based on experimentally observed relationships between parameter would also likely reduce the occurrence of unrealistic combinations while improving the physical representativeness of the simulations.

Additional investigation of the thermal expansion coefficient, α_T, is recommended, particularly regarding experimental measurement methods and uncertainty evaluation. The sensitivity analyses showed that α_T has significant influence on the stress/strength ratio, despite not being directly measured in current Swedish testing procedures. As mentioned, the parameter is adjusted to fit the total measured deformation, which introduces uncertainty into a crack risk simulation. Implementing reliable and standardized methods to directly measure the thermal expansion coefficient in low-clinker concrete could improve the accuracy of crack risk analyses.

Additional studies including other supplementary cementitious materials, such as fly ash or volcanic ash, would broaden the understanding of low-clinker concrete behavior. Such studies could investigate whether the parameter sensitivities observed in this thesis are specific to concrete containing slag or if similar trends can also be identified for other low-clinker binders. However, in order for such a continuation, the Matlab model needs to be further developed and investigated to establish why some parameter combinations resulted in non-real values.

References

Berrocal, C. G., Löfgren, I., Lundgren, K., & Tang, L. (2015). Corrosion initiation in cracked fibre reinforced concrete: Influence of crack width, fibre type and loading conditions. *Corrosion Science*, *98*, 128–139. https://doi.org/10.1016/j.corsci.2015.05.021

Berrocal, C. G., Löfgren, I., Magnusson, J., Mathern, A., Saleh, I., Suchorzewski, J., & Rempling, R. (2024, April). *Metoder för sprickriskbedömning och-begränsning hos hårdnande betong; en omvärldsanalys och parameterstudie (projektnr. 14170)* (tech. rep.). SBUF.

Boverket. (2025, January). Utsläpp av växthusgaser från bygg- och fastighetssektorn. https://doi.org/https://www.boverket.se/sv/byggande/hallbart-byggande-och-forvaltning/miljoindikatorer---aktuell-status/vaxthusgaser/

Byggtjänst, S. (2023). *Ama anläggning 23 : Allmän material- och arbetsbeskrivning för anläggningsarbeten.*

Emborg, M., Bernander, S., Ekerfors, K., Groth, P., & Hedlund, H. (1997, November). *Temperatursprickor i betongkonstruktioner; beräkningsmetoder för hydratationsspänningar och diagram för några vanliga typfall* (tech. rep.). Luleå Tekniska Univeristet.

Engström, B. (2007). *Restraint cracking of reinforced concrete structures* (tech. rep.). Chalmers Tekniska Högskola.

Hedlund, H., Wiberg, H., Nilsson, M., & Persson, M. (2023a, October). *Grönare anläggningsbetong-data för temperatur-och härdningsstyrning slutrapport* (tech. rep.). Luleå University of Technology.

Hedlund, H., Wiberg, H., Nilsson, M., & Persson, M. (2023b, October). *Grönare anläggningsbetong-data för temperatur-och härdningsstyrning slutrapport* (tech. rep.). Luleå tekniska univeristet.

Hedlund, H., Wiberg, H., Rasmark, N., Vogt, C., & Hösthagen, A. (2023, February). *Star-temperatursprickdata för klimatförbättrad betong slutrapport* (tech. rep.). SBUF.

Ji, G. (2008, May). *Cracking risk of concrete structures in the hardening phase: Experiments, material modeling and finite element analysis* (tech. rep.). Department of Structural Engineering, The Norwegian University of Science and Technology.

Khan, M. I., & Siddique, R. (2011). Utilization of silica fume in concrete: Review of durability properties. *Resources, Conservation and Recycling*, *57*, 30–35. https://doi.org/10.1016/j.resconrec.2011.09.016

Krauß, M. (2004, November). *Probabilistischer nachweis der wirksamkeit von maßnahmen gegen frühe trennrisse in massigen betonbauteilen* (tech. rep.). INSTITUT

FÜR BAUSTOFFE, MASSIVBAU UND BRANDSCHUTZ. http://www.digibib.tu-bs.de/?docid=0006364604/08/2016

Löfgren, I. (2024, October). Volcanic ash in concrete, inspired by ancient rome. https://doi.org/https://thomasconcretegroup.com/story/volcanic-ash-in-concrete-inspired-by-ancient-rome/

Löfquist, B. (1946). *Temperatureffekter ihårdnande betong; undersökning av några faktorer som påverka sprickbildningen i grövre konstruktioner - jämförelse mellan två svenska cement* [Doctoral dissertation, Chalmers Tekniska Högskola].

Longlong, L., Ouyang, J., Li, F., Xin, J., Huang, D., & Gao, S. (2018). Research on the crack risk of early-age concrete under the temperature stress test machine. *Materials*, *11*. https://doi.org/10.3390/ma11101822

Naturskyddsföreningen. (2022, February). Cement, klimat, miljö. https://doi.org/https://www.naturskyddsforeningen.se/faktablad/cement-klimat-och-miljo/

Nguyen, D. H., Nguyen, V. T., Lura, P., & Dao, V. T. (2019). Temperature-stress testing machine - a state-of-the-art design and its unique applications in concrete research. *Cement and Concrete Composites*, *102*, 28–38. https://doi.org/10.1016/j.cemconcomp.2019.04.019

Nilimaa, J., Hösthagen, A., & Emborg, M. (2017). Thermal crack risk of concrete structures:evaluation of theoretical models for tunnels and bridges. *Nordic Concrete Research*, *56(1)*, 55–59. https://urn.kb.se/resolve?urn=urn:nbn:se:trafikverket:diva-6070

Nilsson, M., Nilimaa, J., Emborg, M., Hösthagen, A., & Westerholm, M. (2024a). *Analysmetodik och materialmodeller vid inmätning av ung betongs egenskaper för beräkning av temperatur, hållfasthet och spänningar under härdningsförlopp* (tech. rep.).

Nilsson, M., Nilimaa, J., Emborg, M., Hösthagen, A., & Westerholm, M. (2024b). *Materialdata för beräkning av temperatur, hållfasthet och spänningar-betong med anlfa-cement, flygaska och slagg* (tech. rep.). Luleå tekniska univeristet.

Nilsson, M., Nilimaa, J., Emborg, M., Hösthagen, A., & Westerholm, M. (2024c, June). *Spänningsberäkningar, metodik och kriterier* (tech. rep.). Lulå tekniska universitet.

Nilsson, M., Nilimaa, J., & Petersson, M. (n.d.). *Materialdata för beräkning av temperatur, hållfasthet och spänningar uppdrag 20032* (tech. rep.). Luleå tekniska univeristet.

Pinto-Almeida, C., Abril-Camino, A., & Abril-Camino, D. (2025). Mechanical performance of volcanic ash concrete showing modulus reduction with strength retention. *Civil Engineering Journal (Iran)*, *11*, 4422–4435. https://doi.org/10.28991/CEJ-2025-011-10-024

Qu, Z., Zhang, Y., Liu, Z., Si, R., & Wu, J. (2024). A review on early-age cracking of concrete: Causes and control. *Case Studies in Construction Materials*, *21*. https://doi.org/10.1016/j.cscm.2024.e03848

SIS. (2018, August). *Svensk standard ss-en 12390-14:2018* (tech. rep.). Swedish Standards Institute.

Taylor, P. C. (2013, September). *Curing concrete* (1st ed.). Taylor & Francis Group.

Vogt, C., Hösthagen, A., James, G., Panchugin, D., Martin, L., & Mikael, W. (2024, February). *Mätning av töjningar i ung hårdnande betong slutrapport* (tech. rep.). SBUF.

Wahnström, G. (2017, November). *The monte carlo method* (tech. rep.). Chalmers University of Technology.

Wan, Z., He, T., Chang, N., Yang, R., & Qiu, H. (2022). Effect of silica fume on shrinkage of cement-based materials mixed with alkali accelerator and alkali-free accelerator. *Journal of Materials Research and Technology*, *22*, 825–837. https://doi.org/10.1016/j.jmrt.2022.11.110

A

Risk assessment and time plan

Risk Assessment	**CHALMERS**	
Programme: MPSEB	Date: 2026-01-21	Department: Structural Engineering
Student Name: Erik Deborg Victoria Jonasson	Examiner Name: Carlos Gil Berrocal	External Supervisor Name: Ingemar Löfgren Alexandre Mathern Jonas Magnusson
Title of Risk-Assessed Project: Thermal cracking of low clinker concrete		Project Performed at (Company/Workplace/Chalmers): Thomas Concrete Group, NCC, Chalmers

Risk Source	Severity			Action	Responsible	Due Date	Outcome
	Low	Med	High				
General risks of working at an office outside of Chalmers: Risk of fire hazard, noise pollution and ergonomical risks.	☒	☐	☐	Learn and follow the office's safety rules and routines.	Students	First week of the project.	The administrational personnel of the office provided a safety introduction, showing and explaining relevant safety aspects such as evacuation routes and routines in case of emergency.

Students	Examiner	Supervisors
Erik Deborg, Victoria Jonasson	Carlos Gil Berrocal	Carlos Gil Berocal (Chalmers) Ingemar Löfgren (TCG) Alexandre Mathern (NCC) Jonas Magnusson (NCC)

Thermal Cracking of Early Stage Low Clinker Concrete

Starting date	Project duration (weeks)	Version
2026-01-19	21	1.1

		Start	End	Working days	% gjort?
First part		**2026-01-19**	**2026-02-22**	**25**	
1.1	Initial subject research	2026-01-19	2026-01-30	10	70%
1.2	Planning report	2026-01-23	2026-02-06	11	50%
1.3	Theory / Literature study	2026-02-04	2026-02-22	13	0%
Second part		**2026-02-16**	**2026-05-17**	**65**	
2.1	Defining parameters	2026-02-16	2026-03-01	10	0%
2.2	Model verification	2026-03-02	2026-03-11	8	0%
2.2.1	OFaT analysis	2026-03-09	2026-04-12	25	0%
2.2.2	Summarize / analyze results	2026-04-13	2026-04-19	5	0%
2.2.3	Sensitivity analysis	2026-04-20	2026-04-26	5	0%
2.3	Monte Carlo simulation	2026-04-27	2026-05-12	12	0%
2.4	Summarize results	2026-05-11	2026-05-17	5	0%
Third part		**2026-05-18**	**2026-06-15**	**21**	
3.1	Discussion / conclusion	2026-05-18	2026-05-24	5	0%
3.2	Presentation	2026-05-25	2026-06-05	10	0%
3.3	Opposition	2026-05-25	2026-06-05	10	0%
3.4	Final adjustments	2026-06-08	2026-06-15	6	0%
3.5	Final hand in	2026-06-15	2026-06-15	1	0%

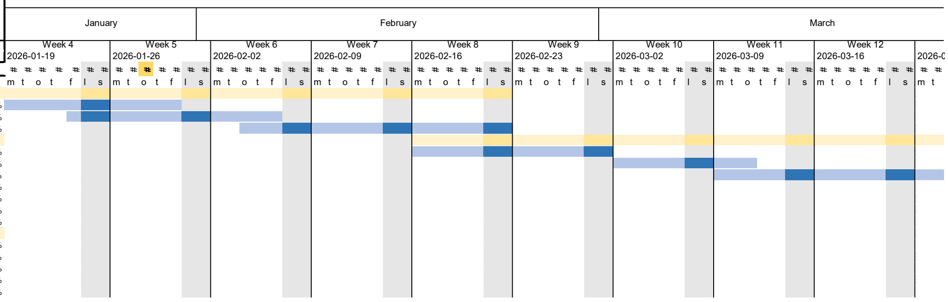

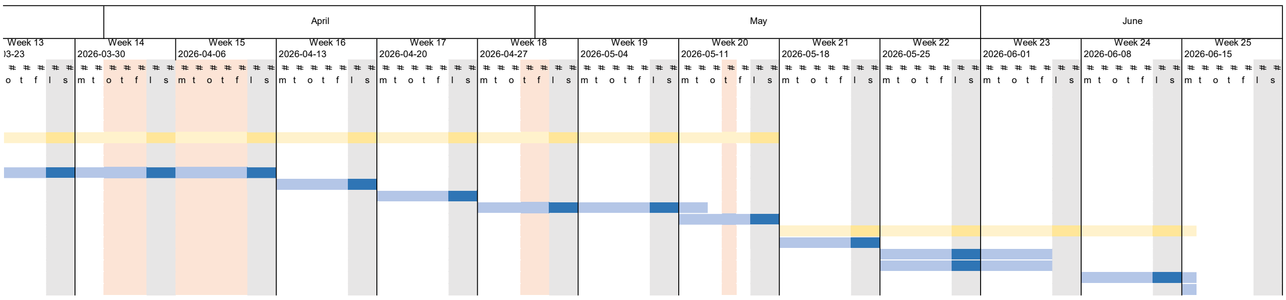

B
Concrete mix composition

Material		Mix 1, ref, [kg/m^3]	Mix 2, 16% slag, [kg/m^3]	Mix 3, 32% slag, [kg/m^3]	Mix 4, 50% slag, [kg/m^3]
Cement	Anl Brevik	320,0	266,6	214,2	156,1
	Anl Slite	80,0	66,7	53,5	39,0
Slag		0,0	63,3	125,8	195,1
Water		168,0	166,6	165,3	163,9
Superplasticizer	Glenium 51/18	2,400	2,380	2,360	2,340
Air-entering agent	MicroAir 105	0,400	0,397	0,394	0,390
0/4 mm Sand		674,1	674,5	674,8	675,0
0/6 mm Gravel		254,8	255,0	255,1	255,2
8/16 mm Aggregates		870,6	871,2	871,5	871,8

Figure B.1: Concrete mix compositions (Nilsson et al., n.d.).

C

Material data

C.1 Concrete parameters

Parameter	**Unit**	**Mix 1, ref**	**Mix 2, 16% slag**	**Mix 3, 32% slag**	**Mix 4, 50% slag**
$t_{e,ini}$	[h]	3.0	3.0	3.0	3.0
$t_{e,fin}$	[h]	5.0	5.0	5.0	3.0
n_{set}	[-]	3.000	3.000	3.000	3.000
$f_{cc,set}$	[MPa]	0.5	0.5	0.5	0.5
$f_{cc,28d}$	[MPa]	56.8	60.0	58.5	52.7
s	[-]	0.162	0.207	0.469	0.525
$n_{cc,28d}$	[-]	0.618	0.671	0.484	0.511

Table C.1: Material data for mix 1-4 regarding strength (Nilsson et al., n.d.).

Parameter	**Unit**	**Mix 1, ref**	**Mix 2, 16% slag**	**Mix 3, 32% slag**	**Mix 4, 50% slag**
θ_{ref}	[K]	4012	4092	4360	5040
κ_3	[-]	0.497	0.373	0.218	0.234
$t_{e,0}$	[h]	0.0	0.0	0.0	0.0
β_Δ	[-]	1.0	1.0	1.0	1.0

Table C.2: Material data for mix 1-4 regarding maturity (Nilsson et al., n.d.).

Parameter	**Unit**	**Mix 1, ref**	**Mix 2, 16% slag**	**Mix 3, 32% slag**	**Mix 4, 50% slag**
$\Delta_{drop,28d}^{max}$	[-]	0.350	0.250	0.000	0.000
$Temp_D$	[°C]	41.0	35.0	21.4	23.4
κ_{Temp}	[-]	1.900	1.900	7.214	9.096
$time_D$	[h]	46.8	46.8	24.0	24.0
κ_{time}	[-]	9.100	9.100	9.029	5.533

Table C.3: Material data for mix 1-4 regarding strength drop (Nilsson et al., n.d.).

Parameter	Unit	Mix 1, ref	Mix 2, 16% slag	Mix 3, 32% slag	Mix 4, 50% slag
W_u	[J/kg]	376000	370000	360000	340000
t_1	[h]	10.000	14.014	20.000	30.000
κ_1	[-]	1.271	1.240	1.150	1.010

Table C.4: Material data for mix 1-4 regarding heat development (Nilsson et al., n.d.).

Parameter	Unit	Mix 1, ref	Mix 2, 16% slag	Mix 3, 32% slag	Mix 4, 50% slag
α_{Heat}	$[10^{-6}/°C]$	11.968	10.251	10.770	12.000
α_{Cool}	$[10^{-6}/°C]$	11.968	10.251	10.770	12.000
k_φ	[-]	2	2	2	2
ε_1	$[10^{-6}]$	0	0	0	0
$t_{s.sh}$	[h]	4.00	4.00	4.00	4.00
ε_2	$[10^{-6}]$	-141.36	-140.59	-141.75	-140.12
t_{S2}	[h]	8.00	8.00	8.00	8.000
t_{s1}	[h]	9.81	8.13	10.00	9.03
η_{SH}	[-]	0.400	0.452	0.600	0.650

Table C.5: Material data for mix 1-4 regarding free movement (Nilsson et al., n.d.).

Parameter	Unit	Mix 1, ref	Mix 2, 16% slag	Mix 3, 32% slag	Mix 4, 50% slag
E_{ref}	[GPa]	34.3	33.4	35.2	33.9
s_E	[-]	0.261	0.365	0.291	0.259
Δ_{t1}	[days]	0.5	0.5	0.5	0.5
a_1 (1d)	$[10^{-12}/Pa\ (^{10}log-unit)]$	8.102	18.000	4.933	15.000
a_2 (1d)	$[10^{-12}/Pa\ (^{10}log-unit)]$	11.065	24.000	15.458	19.000
a_1 (5d)	$[10^{-12}/Pa\ (^{10}log-unit)]$	3.000	4.000	3.800	0.800
a_2 (5d)	$[10^{-12}/Pa\ (^{10}log-unit)]$	3.125	2.371	0.300	0.600
a_2 (14d)	$[10^{-12}/Pa\ (^{10}log-unit)]$	6.920	7.398	4.000	5.000

Table C.6: Material data for mix 1-4 regarding elastic modulus and shrinkage (Nilsson et al., n.d.).

Parameter	**Unit**	**Mix 1, ref**	**Mix 2, 16% slag**	**Mix 3, 32% slag**	**Mix 4, 50% slag**
f_c^{ref}	[MPa]	56.8	60.0	58.5	52.7
f_t^{ref}	[MPa]	3.25	2.94	2.29	2.29
β_1	[-]	0.667	0.667	0.667	0.667
α_{ct}	[-]	0.525	0.825	0.850	0.850
ρ_T	[-]	0.250	0.000	0.630	0.630
ρ_φ	[-]	0.000	0.000	0.000	0.000
Ajd_{Relax}	[-]	1.000	1.000	0.900	0.985

Table C.7: Material data for mix 1-4 regarding tensile strength and stress (Nilsson et al., n.d.).

C.2 Spectrum of relaxation

The spectrum of relaxation for mix 1-4 are presented in Table C.8, Table C.9, Table C.10, Table C.11. The columns in the spectra describes ages at the time of loading, at 0.124, 0.275, 0.39212, 1.24, 3.92, 12.4, 39.212, 124, 392.12 and 1240 days. The rows in the spectra describes the time of retardation, meaning time of loading and are 0.005, 0.05, 0.5, 5, 50, 500, 5000 and 10^{30} days (Nilsson et al., n.d.).

0.01	1.5617	2.9162	3.542	2.1397	2.6981	3.1903	3.5033	3.6921	3.8026
0.01	0.84702	1.2389	1.6106	0.5331	0.66192	0.77625	0.84643	0.88823	0.91244
0.01	0.95823	1.3459	2.1662	2.3801	3.0018	3.5099	3.827	4.0162	4.1265
0.01	1.0734	1.4308	2.8378	4.1059	4.7093	5.2804	5.6537	5.8747	6.0014
0.01	1.0991	1.4475	2.2961	2.6224	2.7433	2.8917	3.0036	3.0835	3.1336
0.01	0.76318	1.0093	1.7605	2.2354	2.4048	2.5542	2.6358	2.685	2.7188
0.01	0.77323	1.0204	1.6958	2.0455	2.1704	2.2904	2.3561	2.3894	2.4065
0.01	-0.28859	0.22475	4.9346	11.757	14.183	15.054	15.501	15.736	15.86

Table C.8: Spectrum of relaxation for mix 1 (Nilsson et al., n.d.).

0.01	0.34104	1.0088	3.8856	4.9086	3.9891	3.3732	3.5182	3.7623	3.9202
0.01	0.24676	0.55582	1.4811	1.7793	1.4689	1.0065	0.86456	0.90386	0.93808
0.01	0.43493	0.74941	1.9008	3.0332	3.2881	3.4193	3.8208	4.0859	4.2434
0.01	0.60418	1.0343	2.3602	3.6702	4.2791	4.9244	5.6271	5.9548	6.1347
0.01	0.85741	1.4374	2.9263	3.5505	3.0482	2.8349	3.0019	3.116	3.1866
0.01	0.64287	1.0826	2.2529	2.8661	2.5876	2.494	2.6441	2.7166	2.7642
0.01	0.6349	1.0668	2.1954	2.7255	2.3938	2.2566	2.3694	2.4185	2.4425
0.01	-0.38256	-0.58963	-0.44757	2.5381	9.9496	14.548	15.441	15.785	15.957

Table C.9: Spectrum of relaxation for mix 2 (Nilsson et al., n.d.).

0.009	1.0435	2.0471	1.5719	1.2346	1.6481	1.9043	2.0381	2.0996	2.1249
0.009	0.63183	0.96927	0.36299	-0.59893	-0.60499	-0.50081	-0.34959	-0.2046	-0.09095
0.009	0.81989	1.2088	1.7941	2.3958	3.0439	3.3071	3.3276	3.2508	3.1592
0.009	0.56717	0.89556	3.3277	5.0922	5.7891	6.1053	6.1244	5.986	5.8157
0.009	0.62631	0.93349	2.2729	2.9112	2.9853	2.9849	3.0012	3.0188	3.0188
0.009	0.45713	0.69692	2.0445	2.829	2.9733	2.9319	2.8314	2.7499	2.7074
0.009	0.50922	0.76776	2.0649	2.7606	2.8598	2.8046	2.6977	2.5881	2.5049
0.009	0.49564	0.98424	4.4966	8.3056	11.035	13.213	14.892	16.13	16.984

Table C.10: Spectrum of relaxation for mix 3 (Nilsson et al., n.d.).

0.00985	1.239	2.4264	4.4848	3.1828	1.8664	1.7	1.7908	1.873	1.9282
0.00985	0.76594	1.1684	1.9252	1.2176	0.10729	0.11645	0.28565	0.34015	0.3535
0.00985	0.84692	1.1795	2.0879	2.6554	2.5511	2.3323	2.2859	2.345	2.4085
0.00985	0.9729	1.3516	2.501	3.9437	4.7233	4.4787	4.2951	4.3568	4.4543
0.00985	1.3122	1.7821	2.8073	3.2824	3.0747	2.7293	2.6181	2.6557	2.7071
0.00985	1.0555	1.4414	2.3715	3.0326	3.0241	2.6199	2.4108	2.3973	2.4296
0.00985	1.1474	1.5628	2.5197	3.0929	2.9892	2.5889	2.3918	2.3695	2.386
0.00985	-0.70755	-0.54012	1.6877	6.7637	13.197	17.741	19.909	20.636	20.874

Table C.11: Spectrum of relaxation for mix 4 (Nilsson et al., n.d.).

DEPARTMENT OF STRUCTURAL ENGINEERING AND BUILDING TECHNOLOGY
CHALMERS UNIVERSITY OF TECHNOLOGY
Gothenburg, Sweden
www.chalmers.se

CHALMERS
UNIVERSITY OF TECHNOLOGY